Sara Filipa Fagulha Pereira

Bachelor in Chemical and Biochemical Engineering

The thermal effects on the methanol-to-olefins reaction: A modelling and experimental approach

TBD: Dissertation submitted in partial fulfillment
of the requirements for the degree of
Master in Chemical and Biochemical Engineering

Adviser: Irina Prokopyeva, Master of Science, Delft University of Technology

Co-advisers: Freek Kaptjein, Full Professor, Delft University of Technology

Isabel Fonseca, Associate Professor, NOVA University of Lisbon

Committee:

Chair: Mário Eusébio, Auxiliar Professor, NOVA University of Lisbon

Raporteur: Inês Matos, Auxiliar Researcher, NOVA University of Lisbon

Member: Isabel Fonseca, Associate Professor, NOVA University of Lisbon

FACULDADE DE CIÊNCIAS E TECNOLOGIA
UNIVERSIDADE NOVA DE LISBOA

September, 2015

The thermal effects on the methanol-to-olefins reaction: A modelling and experimental approach

To my father, who taught me how to count
To my wonderful grandmother
Always and forever to my sister

Acknowledgements

I would like to take this opportunity to firstly thank Prof. Freek Kapteijn and Prof. Isabel Fonseca, for making this last months in the Catalysis Engineering group possible, where I have been surrounded by amazing and inspiring people.

To my daily supervisor, Irina Prokopyeva, who I am incredibly thankful for including me in her project and for her constant guidance and motivational words every time when I was in need of them. With no less importance, I thank Jorge Gascon for his availability and help, as well as to Filipe Lopes and Rob Berger, without whom I would have never had the vision to pursue my work on modelling.

To all the CE group, with particular relevance to the people who have been such a huge support, not only in terms of my thesis but also whenever I needed a good laugh. Thank you Constantino Maldonado, Evelien Bos, Honza Gubiš, Martijn van den Hul and Rommy Gobardhan.

To Prof. Mário Eusébio, who has always pushed me to be the most complete engineer that I could have become so far.

From all my heart, I am absolutely grateful for the amazing friends with whom I have shared this joyful adventure, providing me the time of my life: Adrien Machado, Frederico Martins, João Almeida, Manuel Ribeiro, Mariana Cruz, Marina Elisiário and Sofia Ferreira.

To the ones I left behind, I will thank you forever for being by my side throughout this five academic years. João Valentim, Nádia Pedro, Rita Ribeiro, Rita Soares, Solange Marques and Tomás Monteiro - you are such an amazing group of people and I am truly proud to be your friend.

To the most lovable people in my life to whom I am forever thankful to be family with. I thank my amazing grandmother Lurdinhas, for always caring about me and for loving me every single day, nurturing me the best one can do. Moreover, I thank the greatest father on this planet, Rui Pereira, for always being by my side, wiping my tears and putting me back on track. To my grandfather Leonel, who believe in me from the moment I was born to the day he passed away. To my incredible and supporting boyfriend, Tomás Calmeiro, for his eternal love and patience, without whom I would not have finished this chapter of my life. To my mother, Elsa Fagulha, to whom I am sure now that will be fully part of my life from here after. Moreover, I would like to especially thank Soledade Duarte and Bruno Prendi, for loving me like a daughter and for always embracing me in their family.

Last but not the least, to the most beautiful, bright and glorious person I know, my sister Erica Prendi - we will be by each other's side forever.

Abstract

With the projection of an increasing world population, hand-in-hand with a journey towards a bigger number of developed countries, further demand on basic chemical building blocks, as ethylene and propylene, has to be properly addressed in the next decades. The methanol-to-olefins (MTO) is an interesting reaction to produce those alkenes using coal, gas or alternative sources, like biomass, through syngas as a source for the production of methanol. This technology has been widely applied since 1985 and most of the processes are making use of zeolites as catalysts, particularly ZSM-5. Although its selectivity is not especially biased over light olefins, it resists to a quick deactivation by coke deposition, making it quite attractive when it comes to industrial environments; nevertheless, this is a highly exothermic reaction, which is hard to control and to anticipate problems, such as temperature runaways or hot-spots, inside the catalytic bed.

The main focus of this project is to study those temperature effects, by addressing both experimental, where the catalytic performance and the temperature profiles are studied, and modelling fronts, which consists in a five step strategy to predict the weight fractions and activity. The mind-set of catalytic testing is present in all the developed assays.

It was verified that the selectivity towards light olefins increases with temperature, although this also leads to a much faster catalyst deactivation. To oppose this effect, experiments were carried using a diluted bed, having been able to increase the catalyst lifetime between 32% and 47%. Additionally, experiments with three thermocouples placed inside the catalytic bed were performed, analysing the deactivation wave and the peaks of temperature throughout the bed. Regeneration was done between consecutive runs and it was concluded that this action can be a powerful means to increase the catalyst lifetime, maintaining a constant selectivity towards light olefins, by losing acid strength in a steam stabilised zeolitic structure. On the other hand, developments on the other approach lead to the construction of a raw basic model, able to predict weight fractions, that should be tuned to be a tool for deactivation and temperature profiles prediction.

Keywords: MTO reaction - Thermal effects - Fixed bed reactor - Catalytic testing

Resumo

Com a projeção de uma população mundial crescente, a par do percurso contínuo no sentido de um maior número de países desenvolvidos, a futura procura de *building blocks* químicos básicos, como etileno e propileno, deve ser correspondida nas próximas décadas tendo em vista os combustíveis disponíveis. A reação de metanol-a-olefinas (MTO) é um interessante modo de produzir esses alcenos utilizando carvão, gás ou recursos alternativos, como biomassa, a partir de gás de síntese, por sua vez direcionado para metanol. Esta tecnologia tem sido aplicada desde 1985 e na maior parte dos processos utiliza zeólitos, particularmente o ZSM-5. Apesar da sua seletividade não ser tendenciosa para a formação de olefinas leves, é capaz de resistir à rápida desativação por deposição de coque, o que o torna especialmente atrativo no que toca a ambientes industriais; contudo, esta é uma reação extremamente exotérmica, sendo portanto difícil de controlar e antecipar problemas, tais como *runways* de temperatura ou a formação de *hot-spots*.

O maior foco deste projeto cai sobre o estudo desses efeitos de temperatura, ao abordar ambas as frentes experimental, onde a *performance* catalítica e os perfis de temperatura são estudados, e a de modelação numa estratégia de cinco passos. O paradigma de *catalytic testing* encontra-se presente em todos os ensaios desenvolvidos.

Foi verificado que a seletividade para olefinas leves aumenta com a temperatura, apesar de levar também a uma mais rápida desativação do catalisador. Para contrariar este efeito, foram levadas a cabo experiências utilizando um leito diluído, tendo sido possível prolongar o seu tempo de vida entre 32% e 47%. Termopares foram colocados ao longo do leito catalítico, analisando a onda de desativação e os picos de temperatura. Foi realizada a regeneração do leito entre ensaios consecutivos e foi concluído que esta ação é um poderoso meio para aumentar o tempo de vida, mantendo uma constante seletividade para as olefinas leves, ao perder a força ácida numa estrutura zeolítica estabilizada por vapor. Foi ainda construído um modelo básico, capaz de prever frações mássicas, que deverá ser afinado para a desativação e perfis de temperatura.

Palavras-chave: Reação MTO - Efeitos térmicos - Reator de leito fixo - *Catalytic testing*

Contents

List of Figures

List of Tables

Glossary

ATR adiabatic temperature rise.

BET Brunauer–Emmett–Teller.

DME dimethyl ether.

EDS energy-dispersive spectroscopy.

GC gas chromatography.

HPLC high pressure liquid chromatography.

IR infrared.

IZA International Zeolite Association.

MTG methanol-to-gasoline.

MTH methanol-to-hydrocarbons.

MTO methanol-to-olefins.

MTP methanol-to-propylene.

SEM scanning electron microscopy.

TGA thermogravimetric analysis.

TOS time-on-stream.

TPD temperature programmed desorption.

WHSV weight hourly space velocity.

XRD x-ray diffraction.

ZSM-5 Zeolite Socony Mobil-5.

List of Symbols

Notation

a' specific surface area of catalyst particle [m^{-1}]
A area [m^2]
C concentration [mol m^{-3}]
Cp heat capacity [J kg^{-1} K^{-1}]
D dispersion coefficient [m^2 s^{-1}]
$\mathcal{D}$ diffusion coefficient [m^2 s^{-1}]
Ea activation energy
k kinetic constant / mass transfer coefficient [m s^{-1}]
K equilibrium constant [-]
L length [m]
N number of moles [mol]
r reaction rate [mol kg_{cat}^{-1} s^{-1}]
R universal gas constant (= 8.314) [J mol^{-1} K^{-1}]
h individual heat transfer coefficient [W m^{-2} K^{-1}]
S selectivity [-]
t time [s]
T temperature [K]
u superficial velocity [m s^{-1}]
U overall heat transfer coefficient [W m^{-2} K^{-1}]
W mass of catalyst [kg]
X conversion [-]
y gas molar fraction [-]

Adimensional numbers

Bi Biot number [-]
Bo Bodenstein number [-]
Ca Carberry number [-]
Gr Grashof number [-]
Nu Nusselt number [-]

Pr Prandtl number [-]
Re Reynolds number [-]
Ra Rayleigh number [-]

Greek letters

$\boldsymbol{\beta}$ Prater number [-]
$\mathbf{\Delta\ H_R}$ enthalpy of reaction
$\mathbf{\Delta\ P}$ pressure drop [Pa]
$\boldsymbol{\epsilon}$ porosity [-]
$\boldsymbol{\eta}$ effectiveness factor [-]
$\boldsymbol{\gamma}$ dimensionless activation energy [-]
$\boldsymbol{\lambda}$ thermal conductivity [W m^{-1} K^{-1}]
$\boldsymbol{\mu}$ dynamic viscosity [kg m s^{-1}]
$\boldsymbol{\phi}$ Thiele modulus [-]
$\mathbf{\Phi}$ Weisz-Prater criterion [-]

Chemical species

A oxygenate species (methanol and dimethyl ether)
C light olefins (C_2, C_3 and C_4)
G gasoline range hydrocarbons (long paraffins)
M methanol
W water

Subscripts and superscripts

ax axial (in axial direction)
b bulk (when preceded by C) / bed (in any other application)
cross cross section
e external
eff effective
f fluid phase
g gas phase
glass glass material
i internal
in inside
ins insulation material

obs observed
out outside
p particle
r/reac reaction
s surface
SS stainless steel material
tot total
v volume basis
w wall

CHAPTER 1

Introduction

1.1 The Methanol Economy

According to the United Nations' latest report on population growth , it is expected that by the end of the 21st century that the humankind will have reached around 10.8 billion individuals [2]. This projection, hand-in-hand with the fact that the standard of living and consequently the demand for energy is steadily increasing in developing countries, especially China and India, has led to discussions by the scientific community concerning feasible, renewable and alternative energy supplies for the last decades, since it is predicted that, at today's rate of consumption, the oil reserves will last only 40 years more [33, 36]. At the moment, these alternatives include biomass, hydro, geothermal, sun, wind, tides and waves energy, as well as, in a smaller proportion and unconventional use, heavy oil deposits (Venezuela), oil shale/shale gas (United States) and tar sand deposits (Canada) [32]. Naturally, oil, natural gas and coal are still the major sources of energy and fuel, but they are also the precursors for a panoply of chemical building-blocks and daily finished products whose demand will be bigger than its sole use in fuels for transportation [25].

1.2 Methanol-to-olefins

Amongst the multiple precursors of the petrochemical industry, two light olefins are of great relevance – ethylene and, particularly, propylene, as its demand is increasing due to the expanding market for polypropylene [37]. Both olefins are traditionally produced by fluid catalytic cracking, paraffin dehydrogenation and thermal cracking of ethane, propane or naphtha [43]. However, since the 1970s, an alternative reaction - methanol-to-hydrocarbons (MTH) - is gaining commercial relevance, particularly in China, where this process is being extensively developed and applied [33, 34]. The reason for this stands in having only 1,39% of the world oil reserves, meaning this country cannot depend on this source to shift its

polyethylene negative economical balance to positive values. Therefore, their 13.31% and 1.65% share of the global coal and natural gas, respectively, can be very valuable [33, 34, 43].

The methanol in this reaction is produced through syngas, a mixture of hydrogen and carbon monoxide, both via steam reforming, natural gas or from coal gasification [36]. In its turn, depending on the catalyst and/or the operation condition, the methanol in an equilibrium mixture with water and dimethyl ether, is processed catalytically through a hydrocarbon-pool mechanism, to either gasoline (methanol-to-gasoline (MTG)) or olefins (MTO) [34, 36].

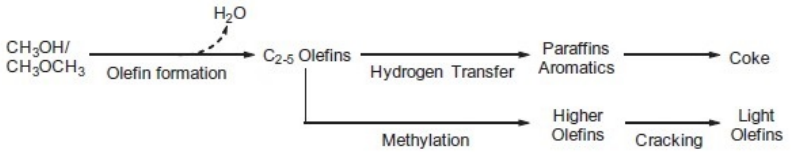

Figure 1.1: The methanol-to-olefins scheme of reactions [40]

The MTO process can be perceived as the further study of the Exxon Mobil's MTG in the 1970s, which gained momentum with the first and second oil crisis [34]. This technology works with both fixed and fluidized beds, of an acid and alumina-based catalyst, where the methanol sets contact, dehydrates to dimethyl ether and then into olefins and other species, like aromatics, naphtenes, higher alkenes and n/iso-paraffins [8, 34]. The operation conditions of Mobil's process is of 400 °C and pressure surrounding the 20 bar, using ZSM-5 as a catalyst [34]. Other technologies are already developed and in the market, as the TIGAS process of Haldor Topsoe (MTG), the Mobil's Olefin to Gasoline and Distillate (MTG), the Lurgi's high focused in maximization of propylene (methanol-to-propylene (MTP)) and also the UOP and Norsk Hydro (now INEOS) MTO's process, using H-SAPO-34 as a catalyst, enhancing the selectivity towards light olefins [25, 34].

1.3 Zeolites as catalysts: ZSM-5

Zeolites are robust and crystalline three-dimensional frameworks, namely microporous aluminosilicates built on tetrahedrons TO_4 (SiO_4 or AlO_4^-), connected between them through the oxygen atoms, forming subunits. These, in their own turn, shape into periodically organized structures, with uniformly sized pores of molecular dimensions (4-10 Å), making them available for diverse applications where they are extensively used as molecular sieves [26]. According to the Database of Zeolite Structures by the International Zeolite Association (IZA), there are 225 framework types, being one of the most important ones the MFI, in which is included the Zeolite Socony Mobil-5 (ZSM-5) commercial zeolite [20]. This zeolite main applications are in heterogeneous catalysis, as for example methanol-to-olefins, methanol-to-gasoline, fluid catalytic cracking, aromatic conversion and other processes [13], having a crystallographic pore diameter of 0.56 x 0.53 nm [24].

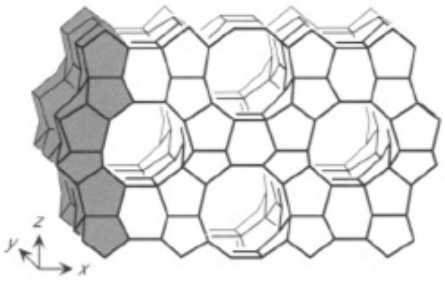

Figure 1.2: Zeolite structures: MFI framework type

The zeolites' selectivity, activity and stability as a catalyst are not only determined by their active sites properties, but also by the dimension and shape of the micropores, openings and channels, which define one of the most important characteristics of these structures: shape selectivity [13]. On the other hand, the activity can be correlated with the strength and localization of the active sites. Nonetheless, even in the case of easy access acid sites, the global activity can be significantly affected by whether diffusional limitations or stereochemical impediments. All these concerns about the activity of the catalyst are strongly linked to deactivation phenomena [13].

Focusing in the reaction of interest to this research project, ZSM-5 is believed to be one of the most suitable for industrial application of the MTO process, not to mention at laboratory scale, mainly because of its high resistance to deactivation by coke deposition and facilitating application as simple fixed-bed reactors [25, 41]. In addition, there are some other inherent advantages of the catalyst, as its 10-ring interconnected channel system, which bestows special shape selectivity, as well as its high catalytic activity and thermal stability [36]. The ZSM-5 zeolite's structure can be modified in such a way that its acid properties are improved and, therefore, the selectivity towards light olefins, because naturally this catalyst has a much lower selectivity when compared to SAPO-34, other broadly zeolite catalyst, in which its framework is found to easily form coke inside [25, 36, 41].

1.4 Literature review: selectivity, activity and modelling in MTO

The research surrounding the methanol-to-olefins and all its particularities is quite extensive, having been found several different fields of interest just for one process.

Starting from the mechanistic studies, more than 20 possible mechanisms have been proposed, encompassing a variety of reactive combinations of molecules and intermediates. An initial approach to this matter by Dessau *et al.* [12] is based on the autocatalytic behaviour of the reaction and in the fact that the presence of small amounts of products enhance the rate of conversion, and so this mechanism would be based on an initial induction period where alkenes would be formed, followed by consecutive methylation, oligomerization and cracking reaction to form aromatics and alkanes. An alternative to this mechanistic proposal is the one by Dahl and Kolboe - the hydrocarbon-pool mechanism. This assumes

the formation of alkenes as an indirect route which uses benzene derivatives, particularly methylbenzenes, as vehicles of propagation. From this aromatic species to alkenes, there are two hypotheses of how it can occur: the paring and the side-chain methylation models. Nevertheless, this is a field in constant research and some alternatives and improvements are being proposed to the established models, as for example the dual-cycle concept, which is the most recent update in this matter as a refinement of the hydrocarbon-pool approach [34].

Another kind of studies is also quite important to address – the kinetics. These include the particular study of the activity, selectivity and lifetime of different catalysts in the MTO reaction, as well as the effect on structural (i.e. defects and shape) [3, 9] and chemical modifications [42] on the process catalyst and even different operational conditions (inlet composition, temperature, pressure, etc.) [41] and used reactors (PFR, CSTR) [31].

In what activity is concerned, this matter has received extensive studies, particularly as its loss can be a consequence coke formation in the catalyst [37]. This is indeed the most important problem to address in the MTO reaction, for the fact it leads to the catalyst deactivation. The parameters that affect this phenomenon, other that the topology of the catalyst itself, are its crystal size, acid strength and acid site density [34, 41]. Both ZSM-5 and SAPO-34 have a medium-high Brønsted acidity, which promotes coke forming reactions, as for example hydrogen transfer and carbenium ion reactions, resulting in polycyclic arenes, paraffins and oligomers, which clog the catalyst's internal channels and the intersections between them [34, 36]. Moreover, the gaseous product molecules or even the dealumination by the water present in the reaction pool can also deactivate the catalysts [16]. As ZSM-5 is a dense zeolite, the deactivation is also associated with gradual coverage of the active sites, and in that case it would be simply considered as a loss of contact time with time on-stream [34]. In spite of this progressive blockage of internal channels, some active sites remain accessible from lateral channels and so deactivation by pore blockage is delayed [36]. Although everything said about deactivation by coke formation, in principle, it is still reversible by combustion at 500-600 °C of the catalyst bed and its activity can be restored [22]. It is important to understand that the regenerated catalyst shows a lower activity than the fresh ones, possibly due to the fact that at elevated temperatures (>500 °C), and in the presence of water, there is some dealumination of the zeolite and, therefore, some active sites are lost and some mesoporosity is gained in the process [17, 22].

Adding the kinetic studies to the study of the deactivation effect, one can also model the process, in order to properly simulate the reactor's performance, which is of great interest in both theoretical and practical aspects [43]. This is of special importance, since, in spite of the considerable technological development of this process in the last decades, the kinetic and temperature modelling are two fields yet to be fully developed, because of the complex reaction scheme of the methanol-to-olefins process [17, 21]. Overall, the kinetic models can be divided in two main classes: the lumped models, where the whole system and diversity of chemical species are simplified to groups of molecules based on their similarity (chemical structure or number of carbons, for example); and the detailed

models, which take in account all the reactions that are found in the hydrocarbon-pool [37].

Moreover, to complete the modelling work, the regeneration step by coke combustion of the catalyst has to be included. With this action, the recovered activity in each regeneration step can be predicted and compared with the initial catalyst activity. Furthermore, as coke combustion is an exothermal reaction and the considered reactor is adiabatic, the evolution of the temperature profiles along the reactor with time can also be simulated and verified by modelling [1, 18]. Nevertheless, the temperature profiles whilst the reaction is occurring and between regenerations, as well as the product and methanol conversion profiles, have not yet been reported. Additionally, the developed modelling for the MTO process still does not include the radial temperature profiles, only the axial temperature dispersion has been simulated. Bearing these challenges in mind, this research project is justified and consequently is focused on the thermal effects of the methanol-to-olefins reaction, enclosing the study of those on the selectivity, activity, lifetime and in regeneration processes.

Chapter 2

Theoretical background

2.1 Catalytic testing

The development of catalysts for new processes, or even for the improvement of existent technology, encloses several progressive stages. The process starts with the combinatorial stages, where several amounts of catalyst formulations are prepared and screened for the best samples, roughly based on their overall performance, including activity, selectivity and stability. In the following steps, the chosen catalysts proceed to a quantification phase, where the kinetic studies, stability tests and eventually scale-up at a pilot plant level, are carried on. Finished this procedure, a new overview over the performance of a specific and especially chosen catalyst is reached. [14, 35]

Nevertheless, the procedure of developing new and/or the optimization of commercial catalysts for a process requires for the already mentioned kinetic studies, i.e the extensive description of reaction rates as function of process variables (temperature, pressure, space-time, feed composition, etc.), to be done. For performing this testing, it is recommended to run experiments during long periods of time on stream so the catalyst stability, and therefore its practical application, can be properly evaluated. [35]

Moreover, other indications exist in order to provide the right catalytic testing set-up and experimental conditions. For example, downscaling is highly recommended, for the fact that it requires smaller and cheaper materials for building the set-up, as well as it involves lower utility requirements and safer experiments, all of this making possible highly accurate experiments. Nonetheless, it is very important that the latter goes hand-in-hand with a right reactor choice, which has to be determined based on the type of information required to extract, operation mode (steady-state or transient), the physical states involved and of course its cost, ease of construction and use. This criteria points to the use of an ideal reactor, such as the plug-flow reactor, particularly fixed-bed ones which are the most widely applied in catalytic testing. This kind of reactor has multiple advantages and helpful

features, as its simplicity, easiness of handling, low related costs, being applicable for both gas and liquid phase systems, as well as that its operation requires little amounts of catalyst to yield primarily conversion data (not kinetic rates). Another one of the major advantages of this kind of reactor is the fact that deactivation is noted directly, which in the MTO reaction shows as a front through the reactor making the moment that all the catalytic bed is fully fouled easily detected. However, some drawbacks can be found, especially when it comes to the possibility of existing temperature and concentration gradients over the stagnant layer surrounding the catalyst pellets, or even the care to ensure that plug-flow behaviour is developed. [30, 35]

Particularly the problem regarding intra- and extra-particle gradients rise from the presence of non-ideal phenomena inside a reactor that should perform in an ideal way [35]. This means that mass and heat transport limitations cannot be neglected and, therefore, they affect the observed catalytic activities and selectivities. Taking a step back, the following are the stages of a catalytic reaction and that have to be considered in all testing experiments [14]:

- Diffusion of the reactants from the bulk fluid to the external surface of the catalyst pellet;
- Again, diffusion through the boundary layer that surrounds the particles;
- Diffusion of the reactant from the pore mouth through the catalyst pores, to the intermediate vicinity of the internal catalytic surface;
- Adsorption of the reactants onto the catalyst surface, followed by reaction and product desorption;
- Diffusion of the products from the interior of the pellet to the pore mouth at the external surface;
- Mass transfer of the products from the external pellet surface to the bulk fluid, passing through the boundary layer once again.

All of the above steps act as a resistance for both transport and reaction, so they can create internal and/or external diffusional limitations in the overall catalytic performance. Some of these limitations can be avoided by playing with some of the catalyst features, as the particle size and shape, and even with the hydrodynamics of the process. Nonetheless, in order to guarantee that accurate measurements of the intrinsic kinetics are extracted from the catalytic testing experiments, there is a series of recommendations and criteria that should be addressed and verified (see Appendix A). [14, 23, 30]

Even if all the required criteria is verified and respected, progressively with time-on-stream the catalyst bed loses its initial activity. This catalytic deactivation adds another level of complexity to the catalytic performance in study, for it affects the correct reading

of the rate parameters and reaction pathways. One can say that, if accounting for the activation factor, the reaction rate law becomes [14]:

$$r'_A = a(t) \cdot k(T) \cdot f(C_A, C_B, \ldots) \tag{2.1}$$

This factor a, in its own turn, is not only a function of time, but also again dependent on the concentration of the diverse species in the reaction mixture in each length of the reactor, having a deactivation kinetic constant of its own. This relation between both catalytic decay and reaction rate complicates the analysis of the catalytic phenomena, especially when it comes to modelling. [14]

2.2 Catalyst deactivation

Focusing on catalyst deactivation, this is one of the major concerns when operating industrial chemical reactors. This phenomenon is extremely complex in terms of the number of reactions and causes that can lead to the activity loss by the catalyst. It is a process of both chemical and physical nature that can occur by a number of different mechanisms, in reactions parallel or in series with the main reaction. The rate of deactivation can vary, according to its origin and process conditions, being clear that the choice of a reactor (fixed-bed, fluidized, slurry, etc.) and the needs for regeneration depend on these, and also on the extent of the deactivation. The study of the field of catalytic deactivation does still face a number of challenges and deserves great attention, because eliminating or limiting the phenomenon leads to catalyst improvement, makes processes more economical and independent from additional capital investment. [4, 15, 29]

The five main mechanisms of deactivation are poisoning, fouling or coking, thermal degradation (sintering, evaporation), mechanical damage and corrosion/leaching. Both poisoning and fouling can be reversed and the catalyst regenerated; and in the case of sintering, evaporation and leaching, the catalytic material should be redispersed or the active sites restored by chemical vapor deposition (CVD) treatment. [29]

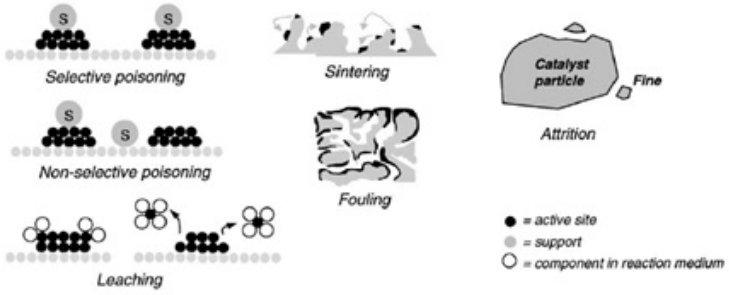

Figure 2.1: Major types of deactivation in heterogeneous catalysis [29]

Poisoning consists in the phenomenon of a strong chemisorption of reactants, products or impurities present in the feed, which leads to the loss of activity of the catalyst by blocking the active sites, reversibly or irreversibly, while modifying their chemical nature

and the overall catalyst performance. However, poisoning can be advantageous, acting as a strategy to shift the selectivity towards some species, although at the expense of the activity. [4, 15, 29]

In the case of the reaction being conducted at high temperatures, thermal degradation can occur, affecting the crystallite shape and dispersion, collapsing of the support structure of the catalyst or even generating some solid-state reactions and transformations of the catalyst phase. Regarding the first mentioned consequence, which is referred to as sintering, it leads to the loss of the active surface and occurs in metal phase-including catalysts, where migration of crystallites or atoms and their coalescence are observed [13]. This deactivation mechanism can occur in all stages of the life-cycle of the catalyst, whether during calcination, reduction, reaction or regeneration. [29]

Considering mechanical failure, this can be observed in several forms, as for example crushing of granular, pellet or monolithic catalyst forms due to a certain load over the bed and attrition between the particles, leading to size reduction and breakup of catalyst granules or pellets to produce fines. The mechanical strength of the particles are dependent of their shape (spherical is preferred) and porosity (macropores in the structure reduces its strength). [4, 29]

Fouling or coking might be the most studied deactivation mechanism. It is also the most frequent in zeolite ZSM-5, when researching about the MTO reaction. This mechanism covers all phenomena where a surface is covered with a deposit (being its origin not always related to the reaction process) and resulting in the loss of the catalyst activity by blockage of the sites, pores, channels and/or intersections [4]. The material involved in fouling can be defined has either carbon or coke: carbon is considered the product of CO disproportionation ($2CO \rightarrow C + CO$), whereas coke has its origin in the decomposition (cracking) or condensation of hydrocarbons. The pathway to coke is rather complex and involve a number of steps, of which the main are the dehydrogenation to olefins, olefin polymerization, olefin cyclization to form substituted benzenes and the formation of polynuclear aromatics from benzene. These reactions proceed via carbenium ions intermediates and are catalysed by the zeolite's Brønsted acid sites [15]. Also, the extent of the reactions depend on the operation conditions (temperature, pressure, partial pressure of steam, composition of the stream, age of the catalyst), affecting therefore the chemical structure of the carbonaceous deposits. Moreover, the coke takes forms that vary from high molecular weight hydrocarbons to primarily carbons, such as graphite and soot [4].

This mechanism of deactivation covers both acid-site poisoning and pore-blocking: at short contact times, coking is relatively slow and deactivation is mainly due to acid-site poisoning; while at long contact times, coking is much faster because of the high concentration of coke precursors. Moreover, if it is the case that the zeolite has small pores or apertures and/or a mono-dimensional structure, deactivation will happen quickly [4, 15].

As it has been mentioned before, the free pathway to access the active sites can be blocked by either direct deposition of carbonaceous species upon the sites and the micropores of the zeolite, or by blocking of the entrance to these micropores, with deposition on the

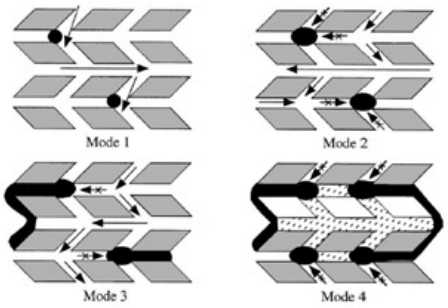

Figure 2.2: Four possible modes of deactivation by carbonaceous deposits in ZSM-5: (1) reversible adsorption on acid sites, (2) irreversible adsorption on sites with partial blocking of pore intersections, (3) partial steric blocking of pores, (4) extensive steric blocking of pores by exterior deposits [4]

catalyst's channels and intersection [22]. The first kind of deactivation is called internal and can be easily found at low temperatures, where the coke is mainly formed by condensation and rearrangement reactions; the second one, which can result from hydrogen transfer reactions at temperatures above 350 °C, is coke deposition in the external surface, having been concluded as the major contributor to catalyst deactivation in the MFI category of zeolites [31, 34]. Internal deposition of coke is hard to analyse from the fact that it is difficult to distinguish the coke precursors from the intermediate species involved in the hydrocarbon-pool mechanism (polymethylated benzenes), being even considered by some researchers that these chemical species can play both roles, depending on their local environment inside the ZSM-5 framework. [3]

All of these concerns regarding whether catalyst testing and deactivation by coke deposition will be thoroughly address through this research project.

CHAPTER 3

Methods and materials

3.1 General set-up description

For the practical part of this research project, the experiments were run making use of a 9 mm of diameter fixed-bed reactor, installed inside the Micrometrics Microactivity Reference unit (PID EngTech®). In Figure 3.1, can be seen a picture of the used set-up, also including the later addition of the three thermocouples system.

This machine provided the different reactions conditions, namely the hotbox and reaction temperature, the nitrogen and methanol flows and proportions, and also the system's pressure. To feed the methanol to the reactor system, an high pressure liquid chromatography (HPLC) pump (307 5-SC-type piston pump, Gilson®) was used. Regarding the effluent stream of the reactor was evaluated throughout the experiment time period by a gas chromatography (GC) device, CompactGC (Interscience®), therefore following the stream's composition in real time, which then made possible to detect the deactivation timing. This apparatus was equipped with a 15 m capillary RTX-1 (1% diphenyl-, 99% dimethylpolysiloxane) column and a flame ionization detector.

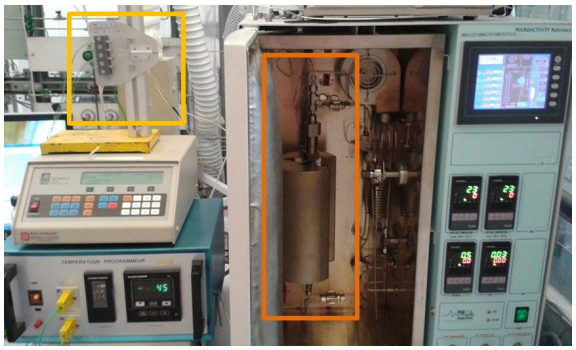

Figure 3.1: Experimental set up - yellow square: arrangement for the three thermocouples; orange rectangle: reactor and its external insulation system, surrounded by the hotbox

3.2 Catalyst preparation

The chosen catalyst for this study was the ZSM-5 CBV 8014 (Si/Al=40) from Zeolyst International®. This zeolite was chosen for the fact of its role in the MTO reaction has been widely studied and can be compared to the current literature, regarding its performance. Moreover, although its selectivity towards light olefins is not as high as, for example, when using SAPO-34, its deactivation is slower, which makes possible longer time-on-stream experiments. Nonetheless, this catalyst is the most extensively used in the industry, making very attractive the concept of better understanding its performance and deactivation profiles in order to draw useful conclusions about how to run under better operation conditions.

The commercial catalyst was pelletized to dimensions between 250 μm (40 mesh) and 425 μm (60 mesh). The resulting pellets were made of use to build the catalytic bed inside the reaction glass tube. Three kinds of beds were created and studied, distinguishing between each other by the amount of silicon carbide (SiC) added: no dilution (purely zeolite), 3:1 and 6:1 (mass basis). These different dilution amounts were used to study the isothermal effect of adding an inert species to the bed. However, one must keep in mind that the mixing of the inert with the zeolite was done by manual agitation, which means that a truly homogeneous bed cannot be guaranteed and the same bed characteristics are not assured between assays.

3.3 Characterisation

A correct characterisation of the catalyst in hands is fundamental for the understanding of its performance during the experiments, and also after its deactivation to verify the extent of coke deposition and the changes in the textural characteristics. From the many existent techniques, the following were selected.

3.3.1 Nitrogen adsorption

One of the most frequently used techniques for the study of the textural aspects of a catalyst is physisorption, namely nitrogen adsorption. This is a quite helpful technique to analyse the micro- and mesoporous structure of the catalyst, as well as to calculate the total surface area and to profile the adsorption and desorption isotherms (including the possible hysteresis effect), which both depend on the particular dimension and shape of the pores. Inside a small range of relative pressures, the Brunauer–Emmett–Teller (BET) analysis can be performed because the adsorption phenomenon is assumed as a modified Langmuir profile, considering both mono- and multilayer adsorption. The experimental data is first fitted with the following expression and for the range of $0,05 < p/p_0 < 0,3$, the amount adsorbed at the monolayer coverage is found and this value can be used to

calculate the total surface area of the catalyst (S_{BET}). [30]

$$\frac{p}{n_{ad}(p^0 - p)} = \frac{1}{n_m C} + \frac{C-1}{n_m C}\frac{p}{p^0} \Rightarrow S_{BET} = n_m A_m N_a \tag{3.1}$$

Where p is the gas pressure, p_0 is the reference pressure, n_m is the amount of gas adsorbed in a monolayer coverage of the zeolite, C is a constant related to the adsorbate-adsorbent interaction, A_m is the occupied area one molecule of adsorbent and N_A is the Avogadro number.

One has to keep in mind that for lower relative pressures, the BET equation is not valid because of the micropore filling, which is diffusion rate dependent, and that some heterogeneity can be observed. In the other hand, at high values of relative pressure, capillary condensation takes place and consequently the BET equation is not valid. [30]

In this research project, adsorption/desorption of nitrogen and associated calculations were performed with the set-up TriStar II 3020 Micrometrics (PID EngTech®) and its associated software. First, the sample was submitted to degassing, where it is submitted to vacuum with nitrogen overnight (16 h) at 350 °C, liberating all the sample surface from previous molecular contamination. In the next morning, the tube containing the degassed sample was then transferred to the nitrogen adsorption set-up. This technique was used on both used and deactivated catalyst.

3.3.2 X-ray diffraction

For the determination of the chemical and crystalline structure of the catalyst, x-ray diffraction (XRD), the powder method, was performed. This technique consists in bombarding the solid sample with X-rays, which are composed of photons resultant from the irradiation of a metallic source, from the incidence of an intensive beam of high-energy electrons [30]. The collection of data results from the elastic scattered ones that are emitted for different angles of incidence of the beam [30].

This technique is developed based on Bragg's law.

$$n\lambda = 2d\sin\theta \tag{3.2}$$

Where n is an integer, λ is the wavelength of the incident X-ray beam, d is the distance between two atomic layers in the crystal (planes of interference), and θ is the angle of incidence and the angle of diffraction. The resulting spectra represents the existent crystalline patterns and relates them with the Bragg angle of incidence.

The XRD patterns of the powders of the fresh catalyst were recorded in Bragg–Brentano geometry with a Bruker D8 Advance® X-ray diffractometer equipped with a LynxEye position-sensitive detector. Measurements were performed at room temperature by using monochromatic CoKα (λ=1,789 Å) radiation between a 2θ of 5° and 50°.

3.3.3 Infrared spectroscopy: pyridine adsorption

In what infrared (IR) spectroscopy is concerned, this is one of the strongest and most important characterisation catalyst techniques, for the fact that it not only displays information about the composition and chemical structures present in the zeolite, as it can also fully identify the acid sites, namely their number, strength and type [13]. This analysis is usually performed using a probe molecule, typically ammonia and pyridine, but nitrogen and carbon monoxides can also be used to extract information on the oxidation state and local environment of the active phase of the catalysts [30].

For this research project, the chosen molecule was pyridine, whose its interaction with the different acidic sites is well studied: when adsorbed on a Brønsted site, it forms a protonated pyridium ion; whereas adsorption on a Lewis site leads to a coordination complex [30].

In this research, the technique was performed by making use of a Nicolet Nexus spectrometer (Thermo Scientific®) at 4 cm^{-1} resolution, equipped with a an extended KBr beam splitting and a mercury cadmium telluride (MCT) cryo-detector. Around 0.05 g of a catalyst sample were pressed at 1132 kg/cm^2 for 5 s to form a self-supporting wafer of 1.5 cm of diameter. The sample was then degassed at 120 °C for 2h under vaccuum (2.10-5 mbar). Pyridine vapour was dosed to the sample stepwise via a known volume and pressure. After each step, the sample was heated at 160 °C to allow diffusion of the probe molecule and, subsequently, cooled to room temperature for spectra collection.

3.3.4 Temperature programmed desorption (TPD)

Another characterisation technique performed was temperature programmed desorption (TPD), which can make a quantitative description of the acid site distribution and the site's strength, essential to correlate the acidity and the catalytic activity of a catalyst, but cannot discern their nature [13].

This characterisation was performed with the help of the Auto Chem II Chemisorption Analyser Micrometrics (PID EngTech®). First, approximately 0.2 g sample were degassed to desorb any adsorbed species on its surface, which was performed under helium flow at the rate of 10 °C/min. This was carried on until 400 °C was reached and then the sample was saturated with ammonia at 200 °C, during 1 h and using a flow of 1.65% NH_3 in helium. Then, the gas mixture was switched back to pure helium and the sample was purged at 200 °C for about 1 h to remove any molecule physisorbed on the surface of the catalyst. At last, a step of 10 °C/min was programmed from 200 °C to 800 °C, also under helium flow, and the ammonia desorption was then followed with a thermal conductivity detector. All flow rates were adjusted to 25 mL/min.

TPD is basically built upon the assumption that each probe molecule is related to one and only acid site, which means that the area below to the TPD curve is proportional to the amount of sites present in the catalyst. A relative analysis of the strength of the sites is also possible, based on the temperature at which ammonia is desorbed. [13]

3.3.5 Thermogravimetric analysis (TGA)

A thermogravimetric analysis (TGA) was executed as well, with the main goal of understanding the temperature at which the fresh catalyst collapses, but also to make a quantitative analysis of the coke present in each deactivated sample. This technique was performed by means of a Mettler Toledo TGA/SDTA851® on samples of roughly 20 mg, under flowing 100 mL/min of air at a heating rate of 5 °C/min up to 1000 °C.

3.3.6 Scanning Electron Microscopy (SEM)

Finally, the last characterisation technique performed on both fresh and regenerated catalyst was scanning electron microscopy (SEM). This is a powerful microscopy technique which can give information on particle size and distribution of the active phases, allowing direct observation of the sample particles as well. Its operation is based on the irradiation of the sample with an electron beam which then generates the ejection of secondary electrons from the sample or the backscattering of incident electrons which can be detected by specific detectors inside the chamber. The intensity of the signal produced in the respective detectors by these electrons can be used to generate a topographic image of the sample besides other type of analysis, such as energy-dispersive spectroscopy (EDS), which allows to analyse a sample and identify which chemical elements are present in it. [30]

Images for this dissertation were produced using a JEOL JSM-6010LA SEM with standard beam energy of 10 keV and a Everhart-Thornley® detector. The SEM/EDS analysis (SEM coupled with an EDS system with a silicon-drift detector) was used to confirm the elemental composition of the sample.

3.4 Catalytic performance

3.4.1 Selected experiments and their aim

Two sets of experiments were taken into practice, each one with different experimental conditions and, naturally, distinct goals.

3.4.1.1 First set – lifetime and selectivity: the effect of temperature and dilution

First of all, both the selectivity and overall lifetime before methanol breakthrough were studied. These experiments were carried on with fresh ZSM-5 CBV 8014, in a 0.50 g bed, to three different temperatures: 400 °C, 450 °C and 500 °C.

The experiments that followed consisted in evaluating also those two parameters after introducing the silicon carbide (SiC), an inert solid in the catalytic bed. The temperatures chosen were only 400 °C and 450 °C, for the fact that it is when the effect of the loss of lifetime is expected to be more pronounced, and so in experiments of short time-on-stream it is possible to study the presence of SiC in the bed. Adding this material to the catalytic bed leads to its dilution and hence improves the temperature control in its inside.

3.4.1.2 Second set – temperature profiling and regeneration

For this second group of experiments, the typical set-up for the previous experiment was improved by placing three thermocouples at different heights inside the catalytic bed, making it possible to read the temperatures at its beginning, middle and bottom.

Regarding the chosen temperature for this second set, it was chosen to be 500 °C, at which the selectivity towards light olefins is higher. Although a shorter time-on-stream for such high temperature can be expected, comparing with the other two developed in the first set, this can be overcome by increasing the length of the bed. Moreover, it is also the chosen temperature for the industrial environmental using this technology nowadays [34], which means that experiments using this condition can be much more comparable with what is daily found in the plants using the MTO reaction, specially in what the temperature profiles throughout the bed are concerned.

Nevertheless, between runs of around 50 h time-on-stream (TOS), the catalyst was regenerated by coke combustion with air at 550 °C during 2 h. Both temperature profiles, during the reaction and regeneration runs, were recorded, and these experiments were performed three times each.

After all the experiments were run, the collected data was analysed to verify if the catalytic testing conditions were satisfied, particularly to evaluate if the assumption for plug flow behaviour was valid and what was the extent of pressure drop, heat transport and diffusional (internal and external) limitations, as well as if the amount of bed dilution is acceptable.

3.4.2 Experimental conditions

Both sets of experiments were initialised in the same fashion. Inside the reaction tube the catalytic bed was built, using quartz wool as a support in its bottom and adding the desired amount of zeolite on top. If a diluted bed was desired, a precise amount of silicon carbide was weighted and add to the catalyst powder already inside the reaction tube. The homogeneity of the bed was achieved by carefully shaking the bed. Then, this reaction tube was placed inside a stainless steel tube, which in its turn is surrounded by an external wall, being everything placed inside the hotbox.

There are two thermocouples placed in the basic set-up: one near the middle of the catalytic bed, outside the reaction tube; and another in the hotbox itself. Both of these temperatures are specified with set-points. Moreover, for the second set of experiments, three thermocouples were placed inside the catalytic bed at specific heights: the first one is at 0.5 cm (T_1) from the bed's inlet, the following is 1 cm bellow (T_2) and the last one is 2 cm under the second (T_3). A simple representation of the placement of the three thermocouples in the catalytic bed is shown in Figure 3.2.

Before initiating the reaction, i.e. admitting the nitrogen and methanol (1:1) mixture, the flow had to stabilise in a full cycle of preheating of the hotbox, taking around 2 h, with nitrogen being constantly circulated through the reactor. Then, a mixture of nitrogen

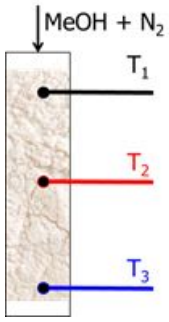

Figure 3.2: Schematic representation of the three thermocouples placement throughout the catalytic bed

and methanol was made and bypassed to be analysed using gas chromatography, so it was guaranteed that the stream's flow and composition was constant and stable, when admitted to the reactor. Moreover, this flow is used to calibrate the system, so it is possible to measure afterwards the amount of methanol that is consumed, as well as it is makes possible to evaluate the selectivity towards the multiple amounts of products.

Each experiment finishes between 10 to 120 hours after the methanol admission to the reactor, depending on the rate at which coke is formed inside the bed, thus this being related with the mass of catalyst, weight hourly space velocity (WHSV), temperature and dilution rate used in each experiment. When the methanol breakthrough was achieved, which is detected by the increase of methanol in the outlet stream by the GC (conversion drops from 100% to 0%), the experiment is disengaged and the data collected.

Particularly in the second set of experiments, there were three reaction runs and between each one the catalytic bed was regenerated.

Both fresh and spent catalyst from the two sets of experiments were submitted to characterization, as it has been thoroughly described in the previous section.

A resume of the experimental conditions for the first set and second set of experiments can be found in Tables 3.1 and 3.2.

Table 3.1: Experimental conditions for the first set of experiments

		Temperature	Pressure	Inlet proportion ($MeOH:N_2$)	WHSV ($g_{MeOH}/g_{cat}h$)	Time on stream	Mass of ZSM-5
	No dilution	400 °C	1.0 - 1.1 bar	1:1	8 h^{-1}	40 h	0.50 g
		450 °C				22 h	
		500 °C				11 h	
Dilution	**3:1**	400 °C				63 h	
		450 °C				35 h	
	6:1	400 °C				63 h	
		450 °C				37 h	

3.5 Modelling

Another important part of this research project consisted in developing a kinetic model that could profile the changing products with time and length of the reactor, as well as

Table 3.2: Experimental conditions for the second set of experiments

		Temperature	Pressure	Inlet proportion ($MeOH:N_2$)	WHSV ($g_{MeOH}/g_{cat}h$)	Time on stream	Mass of ZSM-5
Reaction	**1 st run**	500 ℃	1.0 - 1.1 bar	1:1	4 h^{-1}	37 h	1.75 g
	2 nd run					73 h	
	3 rd run					105 h	
	Regeneration	550 ℃		Air		2 h	

it should include the simulation for the axial and radial temperature profiles inside the catalytic bed, for the different experimental conditions that were performed.

Nevertheless, for the construction of that model, it was chosen as a reference the lumped model proposed by Gayubo *et al.*, where there are eight generic reactions considered, starting from the equilibrium reaction between methanol (M) and dimethyl ether (DME) (D), and passing through the production of light olefins (C) and gasoline range hydrocarbons (G). [16]

$$2M \overset{k_1/k_{1'}}{\longleftrightarrow} D + H_20 \tag{3.3}$$

$$M \overset{k_2}{\rightarrow} C \tag{3.4}$$

$$D \overset{k_3}{\rightarrow} C \tag{3.5}$$

$$2C \overset{k_4}{\rightarrow} G \tag{3.6}$$

$$M + C \overset{k_5}{\rightarrow} G \tag{3.7}$$

$$D + C \overset{k_6}{\rightarrow} G \tag{3.8}$$

Considering the latter reactions, it can also be adapted the following net rate expressions at zero time-on-stream, assuming no deactivation inside the catalytic bed.

- Methanol

$$(r_{\mathrm{M}})_0 = \left[\frac{dX_{\mathrm{M}}}{d(W/F_{\mathrm{M0}})}\right]_0 = \frac{-k_1 {X_{\mathrm{M}}}^2 + (k_1/K)X_{\mathrm{D}}X_{\mathrm{W}} - (k_2 + k_5 X_{\mathrm{C}})X_{\mathrm{M}}}{1 + K_{\mathrm{W}}X_{\mathrm{W}}} \tag{3.9}$$

- Dimethyl ether

$$(r_{\mathrm{D}})_0 = \left[\frac{dX_{\mathrm{D}}}{d(W/F_{\mathrm{M0}})}\right]_0 = \frac{k_1 {X_{\mathrm{M}}}^2 - (k_1/K)X_{\mathrm{D}}X_{\mathrm{W}} - (k_3 + k_6 X_{\mathrm{C}})X_{\mathrm{D}}}{1 + K_{\mathrm{W}}X_{\mathrm{W}}} \tag{3.10}$$

- Light olefins

$$(r_{\mathrm{C}})_0 = \left[\frac{dX_{\mathrm{C}}}{d(W/F_{\mathrm{M0}})}\right]_0 = \frac{k_2 {X_{\mathrm{M}}}^2 + k_3 X_{\mathrm{D}} - k_4 {X_{\mathrm{C}}}^2 + (k_5 X_{\mathrm{M}} + k_6 X_{\mathrm{D}}) X_{\mathrm{C}}}{1 + K_{\mathrm{W}} X_{\mathrm{W}}} \tag{3.11}$$

- Gasoline range hydrocarbons

$$(r_{\mathrm{G}})_0 = \left[\frac{dX_{\mathrm{G}}}{d(W/F_{\mathrm{M0}})}\right]_0 = \frac{k_4 {X_{\mathrm{C}}}^2 + (k_5 X_{\mathrm{M}} + k_6 X_{\mathrm{D}}) X_{\mathrm{C}}}{1 + K_{\mathrm{W}} X_{\mathrm{W}}} \tag{3.12}$$

- Water

$$(r_{\mathrm{W}})_0 = \left[\frac{dX_{\mathrm{W}}}{d(W/F_{\mathrm{M0}})}\right]_0 = k_1 {X_{\mathrm{M}}}^2 - (k_1/K) X_{\mathrm{D}} X_{\mathrm{W}} \tag{3.13}$$

Where k_i are kinetic constants and X_i are weight fractions by mass unit of the organic compounds.

As a consequence of the coke deposition, adjustments on these rates are later performed by introducing the relative catalytic activity in each moment of the experiment: $a = \frac{r_i}{r_{i0}}$. It is also proposed by the authors of this model that this factor for deactivation is partially selective, as it considers the same activity for all the steps of the kinetic scheme except for the first one, the methanol dehydration reaction, which is assumed to be slower than the other steps: $a_{\mathrm{D}} = a^{0.25}$. [16]

Moreover, activity is considered to be the product of recoverable and irreversible activities, being the first related to coke deposition in the zeolite structure and the second with its dealumination by the produced steam in the methanol dehydration reaction [16]. Anyhow, for the span of temperatures used in the experiments, dealumination is not considered for the sake of the simplification of the model. Hence, the activity turns out to become the following expression, being the species A the oxygenates (methanol and dimethyl ether) [16].

$$-\frac{da_{\mathrm{r}}}{d_{\mathrm{t}}} = \frac{k_{\mathrm{dA}} X_{\mathrm{A}} + k_{\mathrm{dC}} X_{\mathrm{C}} + k_{\mathrm{dG}} X_{\mathrm{G}}}{1 + k_{\mathrm{dW}} X_{\mathrm{W}}} \tag{3.14}$$

The next step consisted of taking the above expressions and creating a routine in which the both activation and the mass fractions of the species could be intertwined. The first attempt of doing that was performed in Matlab®, having been successful in the representation of the kinetics and product profiles with space time (length of the catalytic bed), as well as of the activity using the mass fractions at the exit of the bed with time on stream. In spite of having been able to accomplish these first steps, the following ones were not possible to keep on developing. The biggest challenge was to combine the five differential equations for each species involved (which is dependent on space time) with the differential equation for activity (dependent on time-on-stream). Consequently, it was

decided to make a new approach to the model, creating a new routine in Athena Visual Studio 14.0®.

In this new model, not only the above expressions were considered, but also the mass and enthalpy balance to the gas bulk were included (a thorough description on the developed model can be found in [6]):

1. Mass balance in the bulk: accumulation = axial dispersion – convection – reaction;

$$\frac{\partial C_{i,b}}{\partial t} = \frac{\mathcal{D}_{ax,i}}{\varepsilon_b {h_b}^2}\frac{\partial^2 C_{i,b}}{\partial^2 z} - \frac{u_0}{\varepsilon_b h_b}\frac{\partial C_{\mathrm{i,b}}}{\partial z} - \frac{C_{\mathrm{i,b}}}{\varepsilon_{\mathrm{b}} h_{\mathrm{b}}}\frac{\partial u_0}{\partial z} - \frac{W_{\mathrm{cat}}}{A_{\mathrm{cross}}\varepsilon_0 h_{\mathrm{b}}} r_{\mathrm{i}} \tag{3.15}$$

   Where the boundary conditions to solve this equation are the following:

   - Left boundary condition (z=0):

$$\frac{\mathcal{D}_{ax,i}}{h_b}\frac{\partial C_{i,b}}{\partial z} = -\frac{u_{0,f}}{\varepsilon_b}(C_{i,feed} - C_{i,z=0}) \tag{3.16}$$

   - Right boundary condition (z=1):

$$\frac{\partial C_{i,b}}{\partial z} = 0 \tag{3.17}$$

2. Heat balance for the gas bulk including the inert packing between the catalyst particles: accumulation = axial conduction – (axial) convection – heat transfer to the catalyst pellets – heat transfer to the wall;

$$(\varepsilon_b \rho_G C_{p,G} + (1-\varepsilon_b) b \rho_{dil} C_{p,dill})\frac{\partial T_b}{\partial t} = \tag{3.18}$$

$$= \frac{\lambda_{ax}}{h_b^2}\frac{\partial^2 T_b}{\partial z^2} - \frac{C_{p,G}\rho_G u_0}{h_b}\frac{\partial T_b}{\partial z} - \frac{W_{\mathrm{cat}}}{A_{\mathrm{cross}} h_{\mathrm{b}}}\sum_i (-\Delta_{\mathrm{r}} H_{\mathrm{i}} r_{\mathrm{i}}) - h_w A_w (T_b - T_w)$$

   Where the boundary conditions to solve this equation are the following:

   - Left boundary condition (z=0):

$$\frac{\lambda_{ax}}{h_b}\frac{\partial T_b}{\partial z} = -C_{p,G,feed} u_{0,feed} \rho_{G,feed} (T_{feed} - T_b) \tag{3.19}$$

   - Right boundary condition (z=1):

$$\frac{\partial T_b}{\partial z} = 0 \tag{3.20}$$

As a result, a model which simulates the product profiles with time on stream and position in the catalytic bed, and also the activity profiles and temperature for the same variables, was successfully built.

CHAPTER 4

Results and discussion

This chapter includes the analysis of the experimental results and how they are related to the catalytic testing assumptions and conditions, as well as the modelling work developed throughout this project.

4.1 Catalytic testing: assumptions and real conditions

In the Chapter 2, the importance of the catalytic testing mind-set over the engaged experiments was explained. Particularly, its relevance can even be easily underlined through a simple exercise. At the beginning of this research, a preliminary comparison, between our first results of the dependence of selectivity and catalyst lifetime with regards to the operating temperature, and published ones already over this subject, which used ZSM-5 as a catalyst with a similar Si/Al ratio, was performed. This revealed a clear incongruence between the two (Table 4.1).

Table 4.1: Resume some results from literature regarding catalyst lifetime

Source	Reference	T (°C)	Reactor diameter (mm)	WHSV ($g_{MeOH}/g_{cat}h$)	Lifetime (g_{MeOH}/g_{cat})
Choi *et al.*, Nature	[10]	400	13	11	1188
Michels *et al.*, ACS Cat.	[27]	350	-	9.5	304
Michels *et al.*, ACS Cat.	[27]	520	-	2.1	100
Zhang *et al.*, Ind. Chem. Res.	[42]	400	-	8	15
Prokopyeva, Pereira	-	400	9	8	216
Prokopyeva, Pereira	-	450	9	8	180
Prokopyeva, Pereira	-	500	9	8	80

For example, the work of Choi *et al.* [10] report a lifetime of the catalyst five times higher than what we observed in this research project for 400 °C, for a close weight hourly space velocity value. Although this paper has been accepted and published by such a renowned journal, it is believed that their results were achieved being far from plug-flow

regime. These authors did not take in account the importance of catalytic testing, and that is quite clear when evaluating their experimental approach. Choi's group used a fixed-bed reactor like in the case of this research project; however, theirs had an internal diameter of 13 mm (in our group it is of 9 mm) and one fifth of the mass it was used as catalytic bed. Clearly, these conditions do not allow plug flow behaviour, even though the pellets size is not mentioned, since the height of the bed is quite small (assuming a standard porosity of 0.38), only 1.05 mm. Those results are not reliable or reproducible, thus justifying the need of developing experiments which respect the catalytic testing conditions, so they can become a reference for future works in this field. Making an overall observation, it is possible to affirm that all the results are dependent not only of the reaction temperature and weight hourly space velocity, but also on the reactor and bed design (e. g. internal diameter and bed height).

In order to reach those trustworthy and reproducible results, one must assure that is working in a combination of conditions which are within perfect catalytic testing requirements. Those include a set of expressions and span of accepted values that govern plug flow behaviour, allow to neglect axial dispersion, guarantee that the amount of dilution agent is appropriate so no bypassing of the catalyst can happen, and many other assumptions (see Appendix A). The summary of those calculations for both set of experiments developed can be found in Table 4.2, having been considered a constant methanol conversion of 99.14%, resulting in observed rates of reaction of 0.6 and 0.3 $mol_{MeOH}/kg_{cat}s$ for the first and second sets of experiments, respectively.

Making a comprehensive glance over the results, one can firstly realise that not in all developed experiments the criterion for plug flow behaviour was respected. In fact, that was respected in the cases of a high dilution degree and in the three thermocouple experiments.

Moreover, Reynolds, Sherwood and Nusselt numbers are quite close to each other between experiments, which can indicate that not only the developed flow (laminar), but also the mass concentration and heat gradients, are equal between the different sets of experiments.

As expected, the Peclet number differs a great amount in each different experiment. Being directly related with the quality of the heat transfer conditions, the Peclet number is a reflection of the limitations regarding this parameter, thus it is as expected, as higher as the dilution degree or the length of catalytic bed (mass of ZSM-5) is.

Furthermore, the pressure drop for the experimentation systems used is not relevant in any case, surrounding values of the order of magnitude of the millibars. Other parameters in which one cannot perceive much difference between experiments are the internal and external efficiency factors. Those are directly related with the mass transfer gradients and conditions, in which it has been already concluded that those do not vary greatly between different experiments. Particularly, regarding the external efficiency factor, its value is always of 100%, meaning that no external mass transfer limitations are observed in any experiment. On the other hand, internal mass transfer efficiency is consistent within the first set of experiments (62%), but is slightly lower that the value found for the second

Table 4.2: Resume on the catalytic testing calculations for all the developed experiments

		No dilution			Dilution				3TC
		400 °C	450 °C	500 °C	400 °C		450 °C		500 °C
					3:1	6:1	3:1	6:1	
	Re	0.36	0.34	0.32	0.36	0.36	0.34	0.34	0.56
	Pe	20.16	19.12	18.21	42.24	64.32	40.07	61.03	109.93
	Bo	0.50	0.48	0.45	0.50	0.50	0.48	0.48	0.77
	Sh	2.01	1.98	1.95	2.01	2.01	1.98	1.98	2.27
	Nu	1.04	1.02	1.00	1.04	1.04	1.02	1.02	1.25
	ATR (°C)	200.47	160.99	100.94	200.47	200.47	160.99	160.99	100.94
	Pressure drop (bar)	$7.94 \cdot 10^{-4}$	$8.90 \cdot 10^{-4}$	$9.89 \cdot 10^{-4}$	$1.66 \cdot 10^{-3}$	$2.54 \cdot 10^{-3}$	$1.86 \cdot 10^{-3}$	$2.84 \cdot 10^{-3}$	$6.72 \cdot 10^{-3}$
	η_i	0.62	0.62	0.61	0.62	0.62	0.62	0.62	0.74
	η_e	1	1	1	1	1	1	1	1
	Plug flow assumption	Not allowed: 32.59 $\not>$ 75.92	Not allowed: 32.59 $\not>$ 79.90	Not allowed: 32.59 $\not>$ 83.80	Not allowed: 68.29 $\not>$ 75.92	Allowed: 103.99 $>$ 75.92	Not allowed: 68.29 $\not>$ 79.90	Allowed: 103.99 $>$ 79.90	Allowed:114.05 $>$ 49.69
Mass transfer limitations	**External Ca**	$3.06 \cdot 10^{-3}$	$2.94 \cdot 10^{-3}$	$2.84 \cdot 10^{-3}$	$3.06 \cdot 10^{-3}$	$3.06 \cdot 10^{-3}$	$2.94 \cdot 10^{-3}$	$2.94 \cdot 10^{-3}$	$1.22 \cdot 10^{-3}$
	Internal WP criterion	1.29	1.34	1.38	1.29	1.29	1.34	1.34	0.69
Heat transfer limitations (ΔT)	**Internal (K)**	$6.55 \cdot 10^{-2}$	$6.23 \cdot 10^{-2}$	$5.56 \cdot 10^{-2}$	$6.55 \cdot 10^{-2}$	$6.55 \cdot 10^{-2}$	$6.23 \cdot 10^{-2}$	$6.23 \cdot 10^{-2}$	$1.22 \cdot 10^{-2}$
	External (K)	10.90	9.64	8.03	10.90	10.90	9.64	9.64	3.19
	Radial (K)	153.01	136.23	114.34	58.97	35.15	52.17	30.99	56.76
	Axial	229.06	208.63	178.98	165.98	126.70	152.85	117.48	197.68

This table is based on the results obtained through the Eurokin's spreadsheet Fixedbed.xls

set (75%). Thus this can mean that, if the dilution or temperature does not influence this number in the first set, the only two possible parameters responsible for the increasing of the internal efficiency factor are the amount of catalyst used to build the catalyst bed, which instead of the 0.5 g of the first set of experiments, this value was increased to 1.75 g; as well as the methanol flow over the catalyst bed, which is lower, passing from one set to the other from 7 g/h of a value of 4 g/h. The first is not a determinant factor, however when the mass flow is lower, the time for molecule diffusion is increased and therefore the effect over the efficiency factor is directly observed.

The previous affirmations can be corroborated with the results regarding the Carberry number and the Weisz-Prater criterion, which are measures of the internal and external mass transfer limitations, accordingly. Inside the first set of experiments, it is observed that, with increasing temperature and dilution degree, both parameters are influenced in different ways: the external mass transfer limitations slightly decrease and the internal ones slightly increase. These changes are not of a great magnitude and, therefore these results are in accordance with the previous conclusions. Nonetheless, when shifting to the second set of experiments, it is observed that both internal and external mass transfer limitations decrease, most probably again by the fact that the mass flow rate is almost half of the one used in the first set, hence why a higher concentration can be found in the surface and bulk.

Now considering heat transfer related parameters, not only the heat transfer limitations but also the adiabatic temperature rise (ATR) were verified for all the developed experiments. In what those parameters are in account, it is important to mention that those included an analysis for of internal, external, radial and axial degrees of temperature estimated to be present in the system. For all the experiments developed in the first set, only no internal heat transfer limitations (within the pellets) were present, all the others existed. Moreover, that with increasing temperature, these limitations are diminished, possibly given the fact that the hydrocarbon-pool is in its whole exothermic. Not only temperature has this effect over the considered parameters, also when the dilution degree is increased the radial and axial temperature differentials get lower, is a direct and expected consequence of adding an inert to the bed by dispersion the heat generated by the reactions. On the other hand, no difference was observed in the internal and external heat transfer limitation with any dilution degree. Making an overall observance, in all the developed experiments the internal heat transfer limitations were small enough to be accepted, as well as for the second set the external one are also admitted. In all the other cases, the temperature differentials are not admitted.

Regarding the ATR parameter, one can conclude by the resemblance between the values for two sets that this parameter is only a result of the temperature of operation, for the same system of reactions and according enthalpies. Besides, one can conclude that the higher the temperature of operation, the lower the adiabatic temperature rise is, this being a consequence of a lower enthalpy of reaction, which is caused by the shift on selectivities for the same reaction pool.

In order to fully comprehend this matter, one must account for the most relevant and representative reactions of the hydrocarbon pool mechanism, bearing in mind the common products obtain in both sets of experiments developed. Therefore, for the calculation of the enthalpies of reaction for the three different operation temperatures, the following reactions were considered.

- Reaction 1 (R1): ethylene formation (light olefins category)

$$2CH_3OH \rightarrow C_2H_4 + 2H_2O \tag{4.1}$$

- Reaction 2 (R2): propylene formation (light olefins category)

$$3CH_3OH \rightarrow C_3H_6 + 3H_2O \tag{4.2}$$

- Reaction 3 (R3): propane formation (light alkanes category)

$$3CH_3OH + H_2 \rightarrow C_3H_8 + 3H_2O \tag{4.3}$$

- Reaction 4 (R4): butylene formation (light olefins category)

$$4CH_3OH \rightarrow C_4H_8 + H_2O \tag{4.4}$$

- Reaction 5 (R5): methylbenzene formation (aromatic species/coke intermediates category)

$$7CH_3OH \rightarrow C_6H_5CH_3 + 7H_2O + 3H_3 \tag{4.5}$$

- Reaction 6 (R6): heptane formation (long chain alkanes category)

$$7CH_3OH + H_2 \rightarrow C_7H_{16} + 7H_2O \tag{4.6}$$

Additionally, taking the selectivities from the results of the developed experiments at different temperatures with no dilution, it is possible to calculate the enthalpies of reaction, starting from the enthalpies of formation for each species and the standard enthalpy of reaction for each one of the mentioned above. These calculations be found in the Appendix C and a resume can also be found below in Table 4.3.

With the above calculations, one can easily identify the reason why the global enthalpy of reaction of the methanol-to-olefins system decreases with temperature and, therefore, the adiabatic temperature rise decreases as well. That is because increasing the temperature of operation shifts the selectivities of this mechanism towards light olefins (R1 and R2), at the cost of the ones towards aromatics and long chain alkanes. In conclusion, indeed it can be pretty valuable to work at high temperatures, lowering the temperature rise, allowing a better control over the heat transfer limitations (under specific situations, as when adding a dilution agent) and continuing increasing the selectivity towards the most desired products. Nevertheless, one must not forget that coke formation is a concern always

Table 4.3: Resume on the selectivities and enthalpies of reaction (standard and global), for each reaction envolved in the hydrocarbon-pool system considered, for each temperature of operation

		400 °C	450 °C	500 °C	ΔH°_{R} (kJ/mol MeOH)
Selectivities	**R1**	0.05	0.075	0.150	-21.18
	R2	0.125	0.175	0.250	-90.07
	R3	0.200	0.200	0.190	-215.18
	R4	0.125	0.125	0.120	-147.14
	R5	0.250	0.230	0.140	-207.68
	R6	0.250	0.200	0.150	-445.58
Global ΔH_R (kJ/mol MeOH)		-49.81	-47.34	-42.24	

present when working with this mechanism and the ZSM-5 catalyst, and also the lifetime of the catalyst is affected, as a consequence of coke deposition.

Admitting that adiabatic temperature rise refers to the standard temperature of 25 °C, for the second set of experiments that were carried out at 500 °C it can be expected a temperature rise in the catalytic bed of 75.9 °C (calculated by Equation A.4). This prediction was later compared with the real results for this set of experiments, and revealed to be true (Figure 4.9).

Ultimately, the heat transport limitations were evaluated over all perspectives. Inside the pellet, no limitations were found in all the carried experiments. On the contrary, external limitations were present in all experiments, with the exception of the second set. This might be a consequence of a weight hourly space velocity of half the value, which means that almost the double (4 g/h to 7 g/h) the mass of methanol is fed per hour for a bed with a 1.75 g. Therefore, this bed has the sufficient height for heat dispersion to be possible. Radially and axially, heat transfer limitations are always found in each set of conditions applied, which can be related to the high exothermicity of the reactions, hand-in-hand with the a very low global heat transfer coefficient – 1.29 W/m^2K, this is assuming five resistances: the flow inside the reactor, the glass wall of the reactor, the stainless steel insulation outside the reactor, then the external wall which was protecting the system and, at last, the exterior of the system (the interior of the hotbox). These calculations can be found in Appendix D.

4.2 Fresh catalyst characterisation

Over ZSM-5 CBV 8014, some characterisation was performed on this material in order to comprehend its features, regarding acidity, crystalline structure and porosity. Those techniques were extensively described in the previous chapter.

Considering nitrogen adsorption analysis (Figure 4.1), the isotherm resembles one of type II which considers multilayer deposition. A microporous structure is inferred, as well as some mesoporosity, possibly as a result of dealumination by steam in its synthesis step

of this catalyst. Also, the presence of mesopores is supported by the existence of hysteresis in the desorption isotherm, which is of type IV. Both isotherms corroborate the possibility of the pores being in the shape of a rift or a crack. [13]

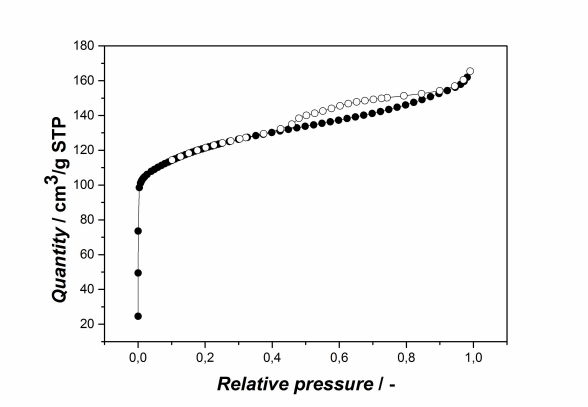

Figure 4.1: Fresh ZSM-5 CBV 8014: nitrogen adsorption and desorption isotherms

From the FT-IR with pyridine adsorption analysis (Figure 4.2), one can observe that both types of acid sites are present. The far left band at 1554 cm^{-1} corresponds to the desorption of pyridine on Brønsted sites, while the far right band at 1455 cm^{-1} is assigned to the pyridine coordination with Lewis sites [7]. Between these two bands, one at 1490 cm^{-1} exists and is related to a mixture of both kinds of acid sites [7]. Moreover, from the area beneath the peaks, one can relatively evaluate the amount of each kind, which is indicating that this zeolite possesses more Brønsted sites than Lewis's, therefore making this catalyst quite adequate for the fact that these type of sites highly maximise the reactions of the methanol-to-olefins reaction pool [24], but are also responsible for the coke deposition [11].

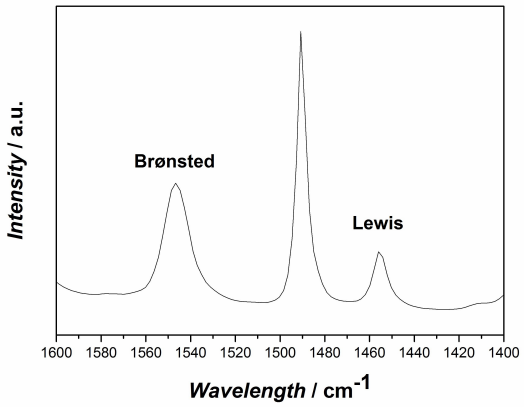

Figure 4.2: Fresh ZSM-5 CBV 8014: pyridine adsorption with FT-IR

Regarding X-ray diffraction (Figure 4.3), the resultant spectrum was compared with a reference given by the IZA database for calcined ZSM-5. From this analysis, it is possible to affirm that no other crystalline phases exist in the commercial catalyst, assuring that one is working with a pure ZSM-5 zeolite.

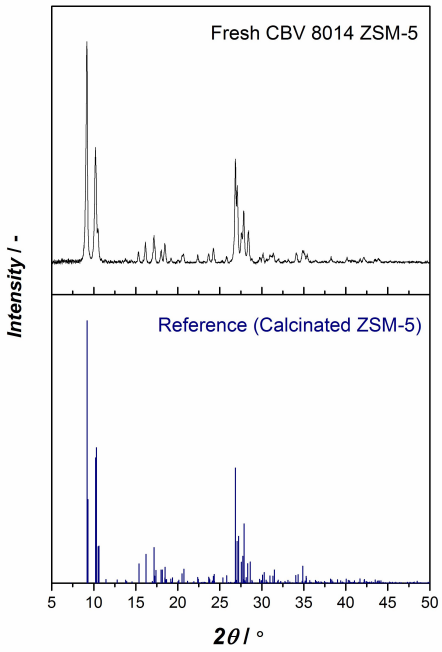

Figure 4.3: Fresh ZSM-5 CBV 8014: X-ray diffraction

Furthermore, to complete the fresh catalyst characterisation, SEM was performed on ZSM-5 CBV 8014 in order to verify the particle's shape and uniformity of their dimension throughout the sample. Considering Figure 4.4, it was found the catalyst in a wide range of sizes, from 0.05 μm to 1μm, but with a roughly consistent spherical shape.

4.3 Analysing the first set of experiments

4.3.1 Selectivity and activity

Making a small remark on this subsection, the methanol conversion with time was always calculated by the following expression 4.7.

$$X_{CH_3OH} = \frac{N_{CH_3OH_{in}} - N_{CH_3OH_{out}}}{N_{CH_3OH_{in}}} \tag{4.7}$$

Moreover, selectivity was calculated by the following expressions based on the reaction's stoichiometry. This list is not complete and exists to provide the line-of-thought of this calculations.

$$S_{lower\ olefins} = \frac{2 \cdot N_{C_2H_4} + 3 \cdot N_{C_3H_6}}{N_{CH_3OH_{in}} - N_{CH_3OH_{out}}} \tag{4.8}$$

$$S_{C_2H_4} = \frac{2 \cdot N_{C_2H_4}}{N_{CH_3OH_{in}} - N_{CH_3OH_{out}}} \tag{4.9}$$

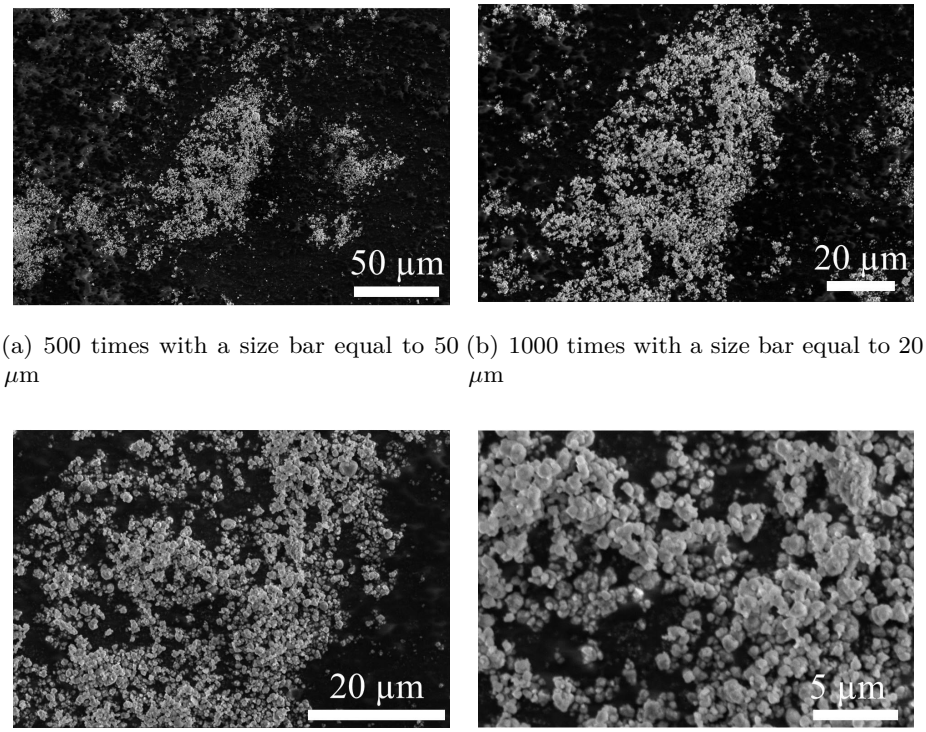

(a) 500 times with a size bar equal to 50 μm

(b) 1000 times with a size bar equal to 20 μm

(c) 2000 times with a size bar equal to 20 μm

(d) 5000 times with a size bar equal to 5 μm

Figure 4.4: SEM pictures of fresh zeolite ZSM-5 CBV 8014 at different zooms

$$S_{C_3H_6} = \frac{3 \cdot N_{C_3H_6}}{N_{CH_3OH_{in}} - N_{CH_3OH_{out}}} \tag{4.10}$$

In this first set of experiments, the catalyst lifetime and selectivity towards light olefins was studied at three different temperatures: 400 °C, 450 °C and 500 °C. Considering Figure 4.5, one can observe that the catalyst lifetime decreases around 10 h with each 50 °C of temperature increment, having been an overall decrease of the catalyst lifetime between 400 °C and 500 °C of around one third (from 27 h to 10 h).

On the other hand, taking in consideration Figure 4.6(a), when the temperature of operation is increased, the selectivity towards ethylene, propylene and butylene increases accordingly, a little over 20% from 400 °C to 500 °C; while the selectivity for light alkanes stays the same (20%) and for the rest of the species, higher alkanes and aromatics, it decreases around 10% (all for the same range of temperatures). Focusing on the light olefins branch (Figure 4.6(b)), it is particularly clear that both ethylene (selectivity increases 10%) and propylene (selectivity increases 13%) are the most temperature influenced species, as butylene keep its selectivity around 12% for all temperatures.

Observing this results, one big concern comes to mind: obtaining higher selectivities towards the product of interest happens at cost of shortening the catalyst's lifetime, which is evidently a sizeable drawback for the process, because it shortens the experimentation

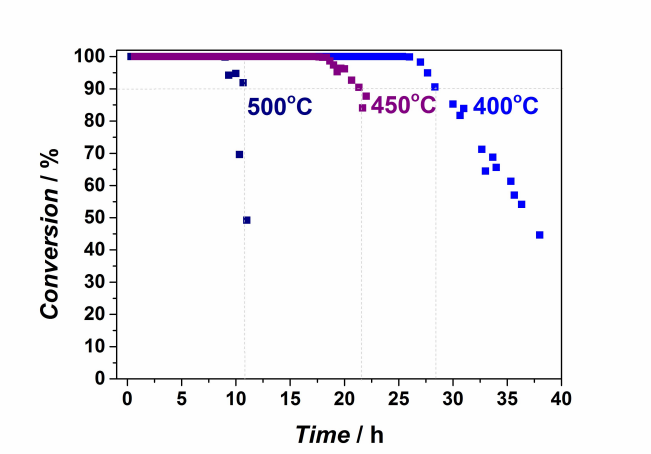

Figure 4.5: First set of experiments: catalyst lifetime for three different temperature, no dilution

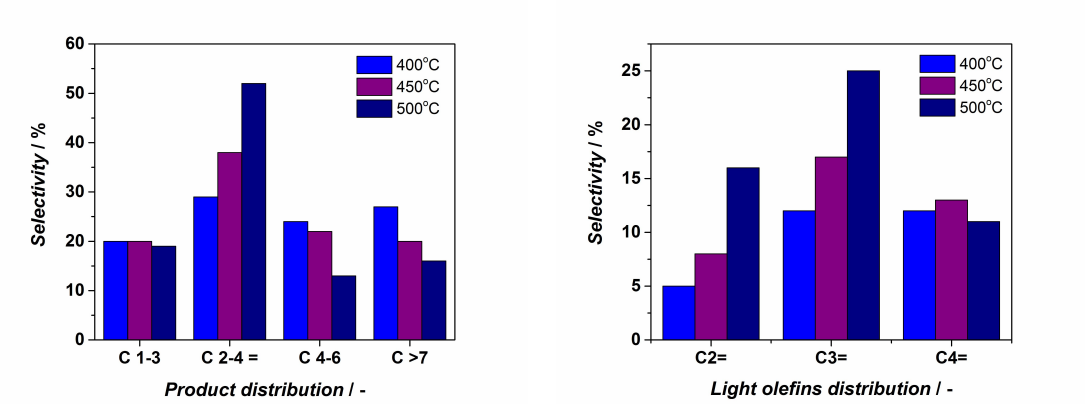

(a) Total selectivity in the develop experiments (b) Close-up in the selectivity towards light olefins

Figure 4.6: Selectivity towards different products for 400 °C, 450 °C and 500 °C (first set, no dilution)

time: more cycles of regenerations per day have to be performed and, ultimately, more money has to be spent purchasing fresh catalyst.

At the end of each experiment at different temperature conditions, a nitrogen adsorption analysis was performed in order to comprehend the effects on the porous structure of the catalyst.

Taking in consideration Figure 4.7(a), when comparing with the fresh catalyst, it is easily detected that a great amount of surface area was lost after each experiment performed, which goes perfectly in line with coke deposition within the catalyst's structure thus blocking it and lessening its area of contact. That loss is quantified to be between 62%-74%.

Moreover, between the samples at the three different temperatures, when making a close-up (Figure 4.7(b)) it is possible to observe that the higher the operation temperature, the higher is the relative surface area, when compared with the other deactivated samples

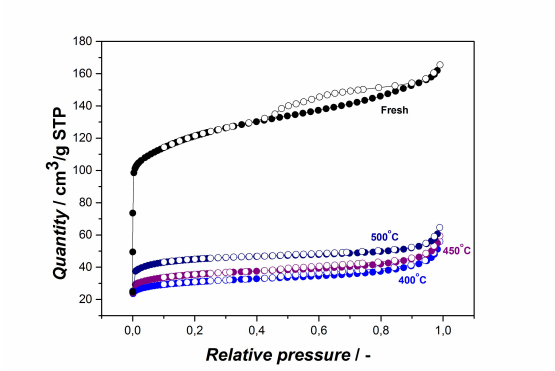

(a) Comparison between fresh and spent catalyst three different temperatures

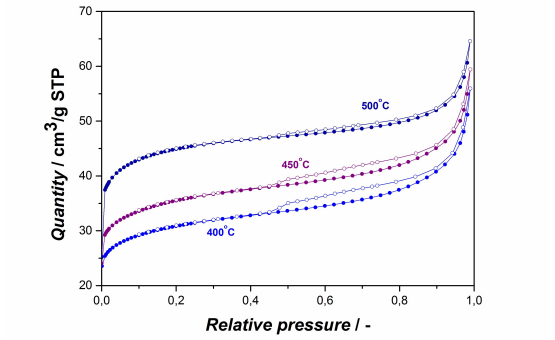

(b) Close-up in the isotherms for the spent catalyst

Figure 4.7: Isotherms of adsorption for fresh and spent catalyst at 400 °C, 450 °C and 500 °C (first set, no dilution) (a), making a close-up over the spent (b)

Table 4.4: Comparison of the catalyst surface area between fresh and spent ZSM-5

Fresh ZSM-5	Spent ZSM-5 @ 400 °C	Spent ZSM-5 @ 450 °C	Spent ZSM-5 @ 500 °C
448 m^2/g	115 m^2/g	133 m^2/g	171 m^2/g

(Table 4.4). Additionally, the hysteresis effect diminishes with increasing temperature. One could think that a lower surface area at lower temperatures would mean that it is at this temperature, per comparison, that the deactivation was stronger. Nevertheless, that is not a true association, and one clear evidence of that is that at lower temperatures, hysteresis is more pronounced, consequently indicating that the sample at 400 °C has a higher mesoporosity compared to the others. This mesoporosity corresponds to the one which already exists when the catalyst is fresh, but is also a consequence of dealumination by the steam formed in the first step of the mechanism (methanol dehydration to dimethyl ether) and internal coke deposition as well. When the temperature of operation is higher, this steam effect is still present in the system yet the pore blockage plays a higher role, particularly externally, making the catalyst lose most of its mesoporosity albeit not affecting most of its microporosity (related to its internal structure). [24]

4.3.2 The effect of dilution

The problem of a shorter lifetime of the catalyst, in order to create the conditions to have a higher selectivity towards light olefins, can be addressed by putting a strategy in practice. This implies the addition of an inert material – in this case, silicon carbide – to the catalytic bed, extending the period in which the catalyst is activated by, particularly considering coke deposition, creating a higher bed for the same amount of catalyst, retarding the methanol breakthrough without affecting the acidity strength and number of sites. This not only increases the catalyst lifetime, as well as it mitigates the temperature effects resultant from the highly exothermic reactions happening inside the reactor.

Bearing this idea in mind, still in the first set of experiments, two temperatures were selected (400 °C and 450 °C) in order to develop experiences with two different degrees of dilution: 3:1 and 6:1, in mass.

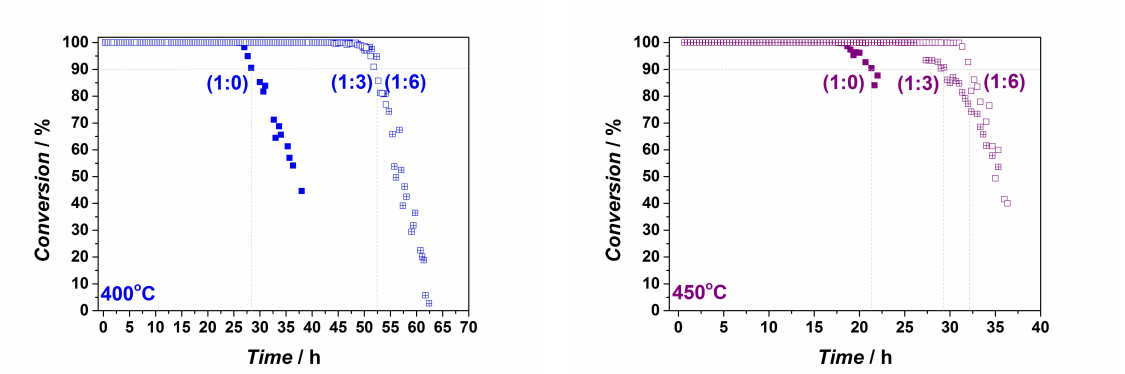

(a) Lifetime of the catalyst for 400 °C

(b) Lifetime of the catalyst for 450 °C

Figure 4.8: Comparison of the catalyst lifetime at 400 °C (a) and 450 °C (b), for dilution degree of 0:1, 3:1 and 6:1 of SiC

With this approach, it was possible to extend the catalyst lifetime to almost two times its value for no dilution, for both temperatures. In the case of 400 °C (Figure 4.8(a)), the catalyst activity was prolonged from 30 h to circa 52 h, while for 450 °C (Figure 4.8(b)) that extension was from 21 h to 29 h - 32 h. Between the two degrees of dilution, no considerable difference was observed regarding the amount of hours in which these were extended because of the particular amount of inert.

Nevertheless, being the case that roughly both 3:1 and 6:1 dilution gave the same effect over the lifetime of the catalyst, under the mind-set of this research project, the calculations regarding catalytic testing for this experiences were observed in detail. Thus, when comparing those for both temperatures, one can conclude that only in the case of the latter the plug flow behaviour assumption is allowed and, indeed, heat transfer limitations are mitigated (namely radial and axial transport), although at cost of a not significant increase in the systems' pressure drop (1.5 times increase, still in the order of the millibars).

4.4 Analysis of the second set of experiments

The second set of experiments involved three consecutive runs at 500 °C and a weight hourly space velocity half the value of the first set (4 h^{-1}), with regeneration steps between them when the catalyst bed was detected to be deactivated. Within the catalytic bed, as it has been thoroughly depicted in the previous chapter, three thermocouples were placed at the inlet, middle and bottom of the bed.

4.4.1 Selectivity and activity

For the first run, when the catalyst was still fresh, an increase in the catalyst lifetime was immediately verified, compared with the homonym run in the first set of experiments. For the first set at 500 °C (Figure 4.9(a)), the total catalyst lifetime was 10 h, while for the second set, the lifetime was extended to circa 33 h, consequence of the double weight hourly space velocity and therefore cutting in half the reaction rate, and being in a verified plug flow behaviour region. Moreover, these new conditions do not especially affect the selectivity towards the multiple analysed species.

Nonetheless, between regeneration cycles, the selectivities change. In fact, although it stays the same for ethylene and propylene after each regeneration, for gasoline range hydrocarbons and paraffins it clearly loses percentage to another olefin, namely butylene. This is easily justified for the fact that, according to the hydrocarbon pool and side-chain paring mechanisms, paraffins are one of the latest groups of molecules formed [34]. After two cycles of regeneration and multiple hours on stream of operation, it is a natural consequence that the catalyst would lose part of its intrinsic acidity and strength, since coke deposition blocks pores and the channels to them, as well as the following combustion leads to the destruction of the overall framework. This assumption will be later verified by material characterization on the regenerated catalyst, in comparison with the fresh one.

4.4.2 Deactivation front and catalyst lifetime

In the early beginning of the second set of experiments, after stopping the bypass to the reactor, the mixture of 1:1 of methanol to nitrogen was admitted. Immediately, it was observed a temperature rise in all three zones along the bed. For the first run (Figure 4.9(b)), this was particularly accentuated at the beginning of the bed, where a total rise in the bed's temperature of around 80 °C in 15 h was detected. During this period of time, all the methanol molecules which entered that slice of the bed were adsorbed and reacted. As the reaction is highly exothermic, it was only natural to observe a considerate increase in that zone, being all the existent acid sites in their complete acidity strength, promoting the mechanism to develop until the last set of reactions, which is mainly paraffin formation [34]. Bearing in mind Table 4.3, the enthalpy of reaction for alkanes is substantially higher in comparison with small olefins, which together with the information from GC that effectively the mechanism selectivity is working in favour of higher alkanes (>C_5 species), are clear

evidences of the assumption regarding the reason for the significant increase of temperature in the first 15 h.

Around that time on stream, it is observed that the temperature in that first zone starts to decrease, therefore displaying the information that no longer any reaction is taking place, hence the first region of the bed is completely deactivated. The same profile is observed for the other two zones, making the travelling of the deactivation front quite clear: methanol adsorbs, gets converted to olefins, aromatics and alkanes releasing heat, and gradually forming coke species which deactivate the region, thus lowering the temperature in a given zone. If one takes a closer look on the results, it is easy to perceive that the deactivation of the middle of the bed actually matches half of the all bed deactivation.

Through this second set of experiments, two regeneration steps were performed between runs, having been studied its effect over the catalyst lifetime and selectivity over the different products of the hydrocarbon pool. Each time, the regeneration step was performed by admitting air at 550 °C, with a volumetric flow of 30 ml/min of a 50:50 (in volume) mixture of air and nitrogen. This action lasted each time around 2 hours, having been observable a quite high increase on the temperature inside the bed, as a consequence of the coke combustion (Figure 4.10). The temperature of 660 °C was reached in the three zones, which is enough the temperature to start observing dealumination of the zeolite's structure [39], compromising its future performance. Particularly, according to literature [5], it would be expected a small loss in the activity of the catalyst when subjected to the regeneration temperature of 550 °C, caused by the deterioration of the Brønsted active sites. This is not observed for the fact that this methanol-to-olefins reaction pool has an extremely high conversion. This matter of regeneration of the ZSM-5 structure will be addressed with more attention in the next section.

Making an overall evaluation of the catalyst performance in this second set of experiments, from the first to the second run the catalyst lifetime was improved from 40 h to circa 80 h, while from the second to the third this was extended to 120 h, thus increasing the catalyst lifetime by three times, relatively at any cost of the selectivity towards light olefins. Adding to this, each time the regeneration was performed, the temperature reached in each run, within each bed slice, was always the same – around 520 °C.

Nonetheless, this is not a strategy to proceed in a longer time operation run, because although lifetime is indeed increased, each time that coke combustion is performed, the framework of zeolite is weakened, affected by dealumination, which destroys the intrinsic acidity of the catalyst and, eventually, leads to its breakage. As a consequence of that, fines can be formed, increasing the pressure drop through the catalytic bed, shifting the operation away from catalytic testing conditions. However, this concerned is less agravated for the fact that the zeolite which has been worked with is more resistant to these consequences, comparing to zeolite Y or mordenite [19], due the steric hindrance of its structure, which limits the condensation of aromatic rings in the internal channels of the catalyst [5].

The regeneration steps have also a great effect over the acidic properties of the catalyst [19]. In fact, it can be possible to affirm that the extended lifetime of the catalyst is both

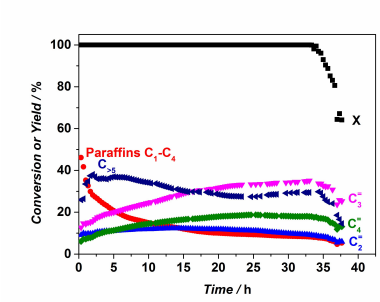

(a) Conversion and selectivities - submited to zero regenerations

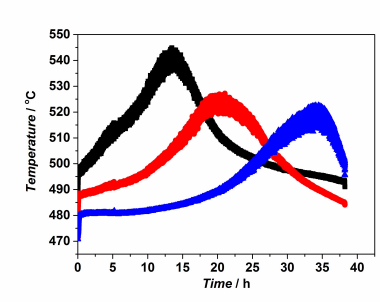

(b) Temperature profiles - submited to zero regenerations

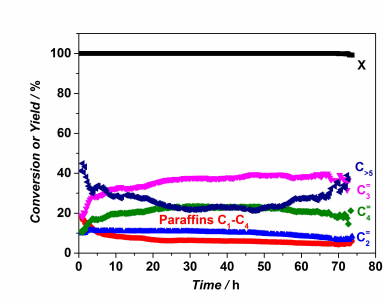

(c) Conversion and selectivities - submited to one regeneration

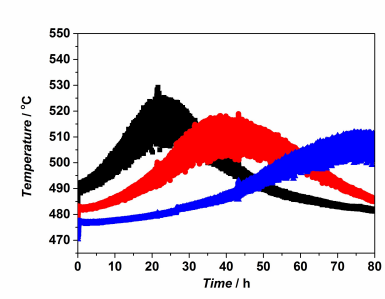

(d) Temperature profiles - submited to one regeneration

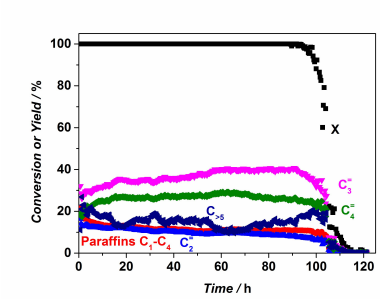

(e) Conversion and selectivities - submited to two regenerations

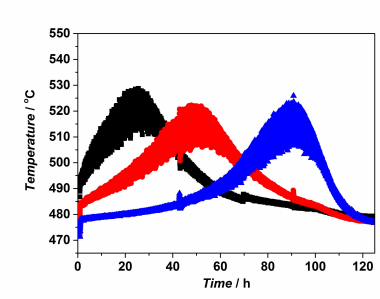

(f) Temperature profiles - submited to two regenerations

Figure 4.9: Study on the effects of regeneration (zero (a,b), one (c,d) and two (e,f)) over the catalyst lifetime and selectivity towards the multiple products; and temperature profiles along the catalytic bed of a 9 mm of diameter fixed bed reactor: black corresponds to inlet, red to the middle and blue at the outlet of the bed

due the dealumination of the structure and also by the loss of the acid strength of the sites, being the latter the main responsible factor. This comes from verifying that no practically no effect is observed on the selectivities.

Still regarding the dealumination topic, the stabilisation of the catalyst could the attributed not to the steam whilst the regeneration steps, but possibly due to the one formed during the reaction time.

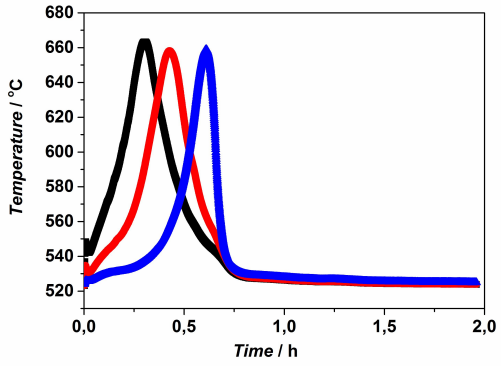

Figure 4.10: Temperature profiles for a regeneration cycle of 2 h at 550 °C

4.4.3 Regeneration

As it has been mentioned before, regeneration steps were performed between runs in the second set of experiments. After the second regeneration, the catalytic bed was collected and analysed through ammonia TPD and TGA, in order to verify its acidic and structural characteristics.

Comparing the fresh catalyst to the one obtained after two regenerations, through TPD analysis (Figure 4.11(a)), it was found that the loss in the number of acid sites was around 81% (Table 4.5). With that loss in number came as well the one in terms of strength, which is perceived by the shift in the temperature of ammonia desorption (from circa 430 °C to 350 °C). Regarding TGA (Figure 4.11(b)), it was performed to understand if any organic mass would still be trapped inside the catalytic structure, but it was found this was not the case.

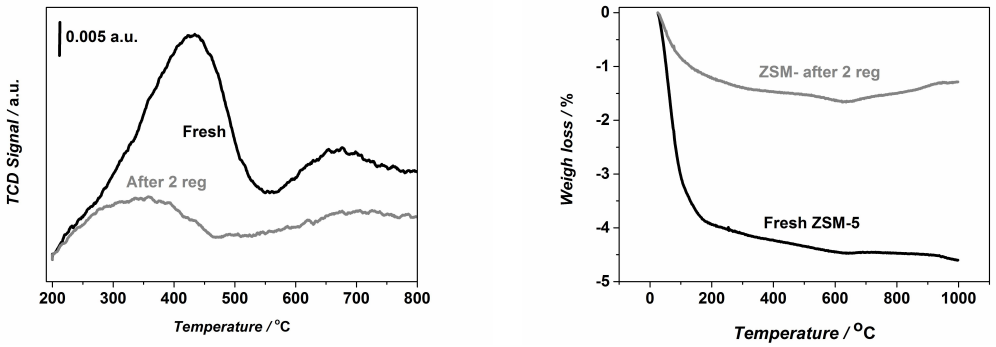

(a) Ammonia TPD analysis

(b) TGA analysis

Figure 4.11: Resume of the characterization on the two-time regenerated ZSM-5 and comparison of it with fresh catalyst

Furthermore, the dealumination of the catalyst structure could be effectively calculated from the TPD resultant information and it was found that the ratio of silica to alumina was increased by five times after both regeneration steps. This in fact means that highly

Table 4.5: Comparison on the acid site acidity between fresh and two-times regenerated ZSM-5

Catalyst	BAS (mmol/g)	SiO_2/Al_2O_3 (from NH_3 TPD)	SiO_2/Al_2O_3 (from Zeolyst)
Fresh ZSM-5 CBV 8014	0.357	90	80
After two regenerations	0.069	488	-

mesoporous and fragile structure was what became out of the initial zeolite's structure. Even the initial ratio of silica to alumina was slightly higher that the reported value from Zeolyst®, which is again related to mesoporosity, in this case created in the zeolite synthesis process. With these results, one can comprehend that, even though regeneration cycles improve catalyst lifetime, this is not an adequate strategy for the reasons mentioned before.

4.5 Modelling

The modelling work developed under this research project has been delimited, from the beginning, in five sequential steps.

First of all, it is essential that one defines all the elementary reaction steps and their rate expressions. It was far most necessary to consider a group of reactions that could be representative of the model that it was intended to build, and that choice has been already depicted in the previous chapter, where both reactions for this lumped model and reaction rate expressions, were defined (Section 3.5).

Based on that, a code using Matlab® was develop, which incorporated those and would print the mass fractions of the different species involved with length of the reactor, for a specific time (Figure 4.12). Those resembled what was observed in real experiments for this reaction, observing the methanol concentration decrease, followed by a small peak on DME, which is then converted to light olefins and gasoline-range hydrocarbons, and disappears. The product profiles stabilise in the beginning of the bed, being kept constant until they leave the reactor.

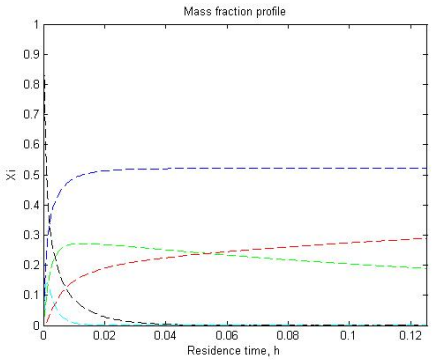

Figure 4.12: Matlab modelling: mass fractions profiles for time zero, function of the length of the reactor. The black curve represents methanol, the dark blue represents water, cyan blue represents DME, green represents light olefins and red is gasoline-range hydrocarbons

Moreover, with an array of mass fractions at a specific length of the bed, it was possible as well to reach the deactivation profile from the inlet to the outlet of the reactor (Figure 4.13). Each curve is representative of the evolution of the activity for a slice of the catalytic bed, being the bottom curve the inlet and the top on the figure the outlet. This result was expected, since that, for a specific time, the fact that the deactivation travels through the catalytic bed as a was whole front, the first slice of bed it's the first encounter of the methanol molecules. These molecules will adsorb and deactivate this first region, but also, as the methanol wave proceeds and progressively deactivates the slices where it passes, less methanol gets converted, until it is observed experimentally the methanol breakthrough.

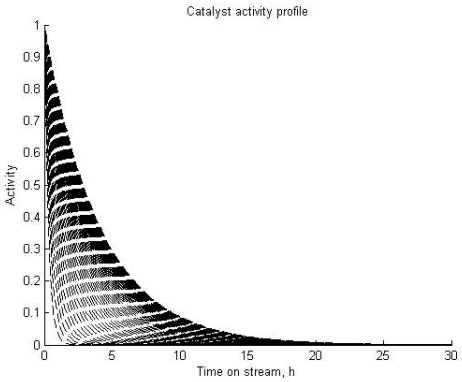

(a) Deactivation profiles for 30 h time-on-stream

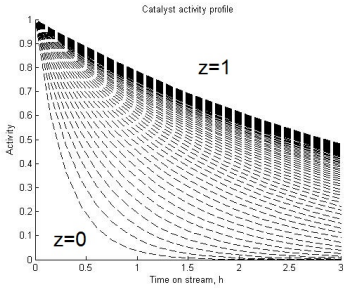

(b) Close-up for the first 3 h of time-on-stream

Figure 4.13: Matlab modelling: catalyst activity as function of time and length of the reactor, based on the fractions at the outlet of the catalytic bed - 500 °C, m_{cat} = 0.5 g, no dilution

From this preliminary results, one could observe the trend on the product composition and relate it to our personal experimental results. With this, one could make a decision about if this considered lumped model from Gayubo *et al.* [16] was adequate to our selectivities and catalyst activity. Indeed, the obtained profiles are comparable, although this preliminary attempt of a model shows a highly fast deactivation of the catalytic bed, which is not whatsoever verified experimentally. For plotting Figure 4.13, the temperature was defined as 500 °C and the mass of the catalyst of 0.5 g with no addition of dilution material. This is basically one of the experiments developed in the first set, where it was found that the catalyst lifetime for this conditions is around 12 h. However, from this model and considering the kinetic constants given by the paper of reference for this modelling work, this lifetime is higher by almost two times (20 h). This simply means that the parameters of the modelling are not tuned for the developed experiments, which should be done later on the modelling process.

At this moment in the five step strategic approach to modelling, both step one (defining all the reactions and expressions involved in the lumped model) and two (defining the expression for quantifying deactivation) had already been reached.

Now, before the important step of defining the boundary conditions and mass/heat

balances, an intermediate step was mandatory. This task consisted of making the weight fractions of the products dependent on both length of the reactor and activity. This part of the modelling strategy was particularly challenging, since the weight fractions are dependent on residence time (i.e. length of catalytic bed) and the expression for activity is dependent on time. Hence combining the five expressions of weight fraction with the one for activation was found to be too time-consuming and another approach had to be done to the model, in order to be able to obtain, for each length of the reactor and each time, the corrected fraction according to the activity in that slice of the bed.

Therefore, the following work on modelling was carried on by Rob Berger[1], who built a one-dimension model, including mass and heat balances to the bed, being able to profile the desired weight fractions with time and throughout the bed.

As to simplifications to be able to build the model, the following were considered.

- All the gas properties keep constant with time and temperature;
- No pressure drop is considered, which is quite accurate based on catalytic testing calculations;
- Spherical particles of uniform diameter;
- No external mass transfer limitations, which is supported by catalytic testing as well;
- No diffusion limitations inside the catalyst particles.

Based on those assumptions, the model was build in two steps. First, a basic one was created in order to incorporate the majority of the parameters and expressions, bearing in mind its continuous refinement every time it was worked on, until ultimately it was reached a point where the model was complete and capable for analysing the dependency of weight fractions with time and length of the catalytic bed.

4.5.1 Model 1 - Base-line

The model which was firstly built (Appendix **??**) had preliminary mass balance and enthalpy balances to the bulk, as well as it includes the activity dependence on temperature, time and longitudinal position in the catalytic bed, allowing this prediction at some extent.

As the balances are a rough first approach and therefore are incorrect, the profiles of weight fraction are not reliable or in any way comparable to what is observed in reality. This prediction can be verified in Figure 4.14, bearing in mind the experimental profiles for selectivity (Figure 4.9), which are directly related to the weight fraction, that were obtained in the second set of experimental work.

Furthermore, all the species show the same trend, increasing progressively with time, although that with higher times-on-stream, the methanol curve does not decrease in such accentuated away, which is followed by a decrease in the other species' weight fractions.

[1]For further professional contact: R.J.Berger@tudelft.nl

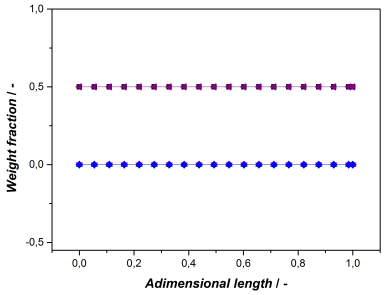

(a) Weight fractions profiles throughout the length of the bed - time 0

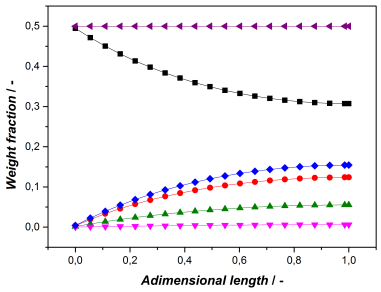

(b) Weight fractions profiles throughout the length of the bed - time 500 s

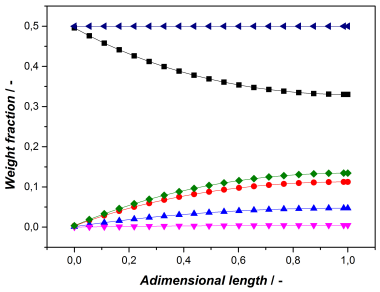

(c) Weight fractions profiles throughout the length of the bed - time 1000 s

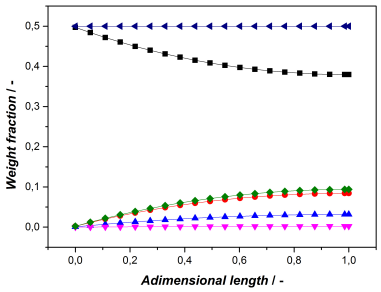

(d) Weight fractions profiles throughout the length of the bed - time 2000

Figure 4.14: Model 1 - Weight fractions profiles on both length of the bed and time (0 s (a), 500 s (b), 1000 s (c) and 2000 s (d)), for the different species considered in the model: black for methanol, red for DME, green for light olefins (C_2, C_3, C_4), pink for gasoline-range hydrocarbons, blue for water and purple for nitrogen

This is caused by the fact that this model considers deactivation, however it considers it from the beginning of the reaction, not allowing for some temporal space where the catalyst wouldn't be coked. In order to corroborate this assumption, one can plot the methanol profiles with time and easily comprehend how with time-on-stream its weight fraction increases (Figure 4.15).

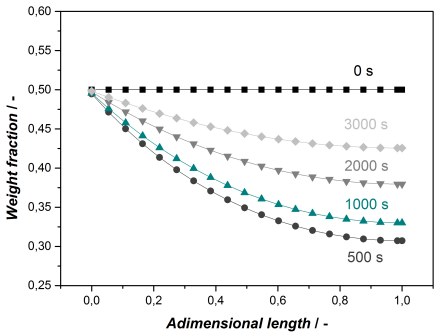

Figure 4.15: Model 1 - Methanol weight fractions with time-on-stream

Nonetheless, although this is a poor model on the methanol-to-olefins product profile estimation, at the same time this can be a means to understand deactivation. Regarding this factor, one can analyse Figure 4.16, and once again comprehend how the deactivation is more accentuated at the beginning of the bed and, with time-on-stream, this difference between the inlet and the rest of the catalytic bed becomes less clear, since all the bed deactivates and so the activity plateaus.

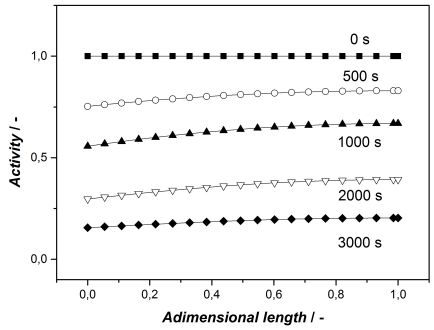

Figure 4.16: Model 1 - Activity dependence on time-on-stream

4.5.2 Model 2 - Complete model (with some restraints)

To reach this model, more than correcting and adding of system parameters, as for example properties of the catalytic bed and dilution conditions, there were other main modifications which should be described in more detail. It was incorporated diffusion limitation, since the reaction rate increases significantly due to the exothermic effect of the reaction. Moreover, enthalpies of formation and reaction were once more calculated and adjusted to the fact that this is a lumped model, and the mass and heat balances were completed. Nevertheless, this more realistic model has some serious convergence problems, which were surpassed by fixating a limit to the reaction rate, making the activity parameter to be fixed (40%) and hence it does not change neither with time or residence time. This catch is directly reflected on the weight fractions profiles (Figure 4.17), which are comparable with the initial ones obtained by Matlab® (Figure 4.12) and also with the observed in the experimental part of the project (Figure 4.9). However, since no change in the activity is produced by the model, no methanol weight fraction is found to change with neither time-on-stream or residence time (Figure 4.17).

It is important to observe that the enthalpy balance continues to be wrong, for the fact that, with increasing TOS, there is no observable difference in the temperature profile throughout the catalytic bed (Figure 4.18), as well as the adiabatic temperature rise in the inlet of the reactor is represented as 200 °C, as in the second set of experiments, where the same temperature is used, it was observed as around 80 °C (Figure 4.9(b)).

From here forward, besides improving and correcting the model that has been built so far, the fourth (redefining deactivation as a function of temperature) and five (parameter

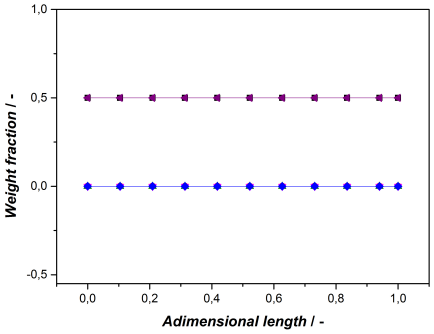

(a) Weight fractions profiles throughout the length of the bed - time 0

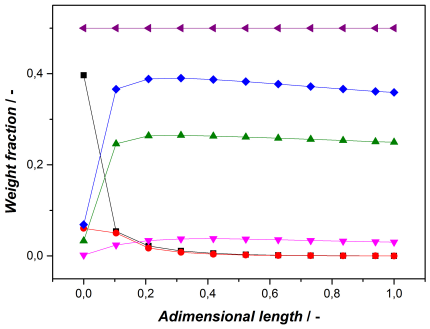

(b) Weight fractions profiles throughout the length of the bed - time 1000 s

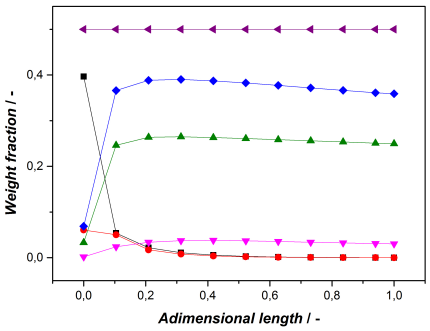

(c) Weight fractions profiles throughout the length of the bed - time 5000 s

Figure 4.17: Model 2 - Weight fractions profiles on both length of the bed and time (0 s (a) and 2000 s (b)), for the different species considered in the model: black for methanol, red for DME, green for light olefins, pink for gasoline-range hydrocarbons, blue for water and purple for nitrogen

fitting with experimental results) steps should be properly developed.

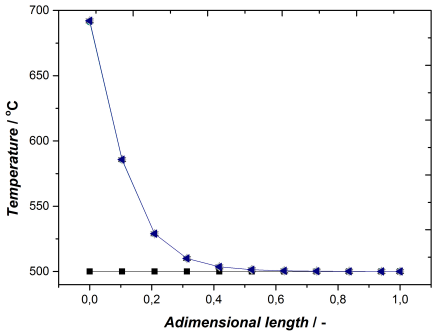

Figure 4.18: Model 2 - Temperature profiles throughout the length of the bed for 0 s, 1000 s, 2000 s and 5000 s

Chapter 5

Conclusions

Especially focused on modelling issues, at the beginning of this research project it was its main goal to find out in the literature what was the best kinetic model that could be adjust to the experimental results using ZSM-5, as well as the further development of this model, that should have included the study of multiple effects (i.e. reactors diameter and operation conditions) over both catalytic performance and temperature profiles. However, throughout the past four months some restraints to this work were found on the way of accomplish it. In this sense, it was firstly built a simple model in Matlab®, from which was possible to observe not only the outlet composition of the gas mixture for the MTO reaction with time-on-stream (TOS), but also the loss of catalyst activity with both TOS and length of the reactor. However, this model was truly very rudimental, including only the operating temperature and mass of catalyst, apart from the kinetic constants. This code could not be further developed thanks to constraints regarding to the combination of multiple partial differential equations dependent on two different variables (time and residence time), and also some because of software issues. Roughly two months were put in effort to continue this work, which afterwards the modelling program was switched to Athena Visual Studio®, where all the parameters regarding the reaction system were incorporated, as well as the proper mass and enthalpy balances.

Within this second approach to the problem, two attempts were built. The first represented false weight fractions profiles, completely distinct from the ones found in the experimental part of the research. This was later concluded to be caused by a incomplete mass balance. However, the effect of loss of activity with temperature and time-on-stream was present and easily represented qualitatively. On the other hand, in the second attempt to develop this model in Athena®, after the mass balance had been corrected, the model became too complex and could only be solved, at that moment, by fixing one value for catalyst activity - 40%. This action lead to a point where the weight fractions profiles were comparable with the initial ones obtained by Matlab® and also with the observed in the

experimental part of the project, albeit the enthalpy balance continued to be wrong.

In the end of all the developed modelling work, it still needs to be validated and tuned with results from the experimental approach of the research project, but it already shows positive and comparable results with the developed experiments, particularly when comparing with the second set.

In spite of the fact that the modelling contribute to this research project was less quantifiable that was expected to be, this approach is on the edge of becoming complete and correct. It affirms itself as an important and scientifically relevant step in the direction of temperature profiles prediction, but a great amount of work has to be done in order to overpass the questions regarding the convergence of the model.

At the same time, the performed experimental work showed quite interesting results and could answer one of the main questions of this research, consisting in how did the different deactivation stages throughout the catalytic bed affect the temperature profiles in its inside, by the innovative approach with the thermocouples.

Making an overall glance, two different sets of assays were carried on with distinct purposes. In the first set, the catalytic performance was studied under the influence of different temperatures and dilution degrees. Regarding the first, as expected from literature, a higher temperature of operation implied a relatively lower lifetime of the catalyst, being this caused by a faster coke formation kinetics promoted by the heat. Not only catalytic lifetime was shown to be affected, but also the selectivity of the products of interest (light olefins) was also affected, in a distinct fashion: the higher the temperature of operation, the higher the selectivity towards ethylene and propylene..

In order to surpass this issue, still in the first set, experiments where carried with the addition of an inert material (silicon carbide), diluting the bed and expectantly improving the catalyst lifetime. In fact, bed dilution was responsible for achieving not only that remark, but also could partially mitigate the temperature effects all through the bed, which is also related to the coke formation. Nevertheless, some limits on the extent of dilution have to be raised in order of not over diluting the bed, which would make the gaseous stream that flows it through to the bed to bypass.

Still on dilution, although the catalyst lifetime achieved was virtually the same for both dilution degrees (3:1 and 6:1), it could have been an assumption that either one can be applicable in further experiments. In fact, it could even thought that, if the effect over the catalytic performance is the same (i.e. same lifetime and no effect over the selectivities), it would be preferable to spend less resources and go for the 3:1 dilution. However, if one remembers, one of the major concerns on this research project was to establish experiments which would conclude in trustworthy and reproducible data, following the proper catalytic testing set of conditions and assumptions. In light of that, calculations for all the carried assays were executed and, thus also these on dilution as well. From the catalytic testing calculations over the matter of dilution, one could understand that, although in practice both dilution result in the same lifetime and selectivity, only when using the 6:1 ratio the experiment was under a valid assumption for plug flow behaviour.

Overall, catalytic testing conditions are a fundamental part of the design of the experimental work, for the fact that these can guarantee that a certain experiment is in conditions where it is not limited by the false assumption of plug flow, so it it would be not subjected to axial dispersion, as well as those inform the researcher about the system limitations, whether if those area related to mass or heat transfer, internally or externally.

Furthermore, the second set of experiments are a fundamental part of this research project and it was where one of the main goals of this work was answered, about the temperature profiles inside the catalytic bed. Effectively, with the placement of the three thermocouples, those were traced and assumptions over the way the deactivation front travels over the catalytic bed, like a breakthrough, were supported. Additionally, with the deactivation of each slice of the catalytic bed, it was observed temperatures rises as in peaks, which each would indicate the full deactivation and coke deposition over the catalyst pores, engaging for the temperature to rise in the next slice of the bed and repeating the cycle.

Between cycles of reaction, two regenerations were performed on the catalytic bed. These procedure had been already found in the current literature as a strategy to improve the catalytic performance at cost of increasing its lifetime. With our results, one could report that this strategy also worked in this project, without affecting the selectivity towards light olefins. It should be taken in account that this is a medium-term solution, since with consecutive regenerations, although ZSM-5 is moderately resistant to dealumination, the catalytic bed become each time more brittle and tending to break its structure. This is caused by the dealumination by steam during the regenerated cycles, and can result in the formation of fines, which introduce a higher pressure drop in the system and, therefore, creates one deviation to catalytic testing conditions. On the other hand, other assumption than dealumination of the structure of being the cause of the increasing lifetime of the catalyst, can be the loss of acid strength, which are in accordance with the results regarding the selectivities being constant after all cycles of regeneration. Adding to this, the steam formation as part of the reaction hydrocarbon-pool is a stabilisation factor for the catalyst, and that can be observed by the disappearance of the higher first peak on the temperature reading, in the following cycles.

In conclusion, all the experiments carried throughout this project have contributed to increase the awareness for the importance of catalytic testing conditions, but particularly in a sense of a new contribute to the scientific community, the results with the placement of the three thermocouples over the catalytic bed were of extremely importance in relation with the deactivation phenomenon. Nevertheless, the modelling work developed so far has shown some results similar to the methanol-to-olefins reaction and it is quite promising after the further steps that need to be taken.

Chapter 6

Recommendations

In this chapter, two categories of recommendations should be included, considering both experimental and modelling work.

Regarding the first, as future prospects in the second set of experiments, some operation conditions should be changing , as other for other temperatures and dilution degrees, in order to understand how do they affect the temperature profiles within and throughout the catalytic bed. Moreover, it was also predicted for this master thesis research project that a new reactor would be received and used for some more experiments related to study the effect of changing the reactor's diameter. With those, it was intended to observe what would become of the heat transfer limitations and, therefore, how would that reflect on the temperature profiles and the deactivation front. Therefore, keeping in mind a more deep understanding of how the methanol-to-olefins reactions is affected by the heat transfer conditions, this suggestion for future experimental work could turn out interesting, especially also if one pays attention not only to the axial temperature profiles but also to the radial temperature profiles.

Bearing that idea in mind, the modelling work should be further developed in order to include these predictions, but also in what comes to incorporate deactivation as a function of temperature. The convergence barrier that has been encountered so far and that does not allow to model the changes in the activation parameter, should be surpassed. Finally, in what modelling is concerned, the model's parameters should be fitted using the experimental results already obtain throughout the last months of laboratory work.

Nevertheless, as future prospects this research project will keep being developed under the doctorate program of Irina Prokopyeva.

Bibliography

[1] A. T. Aguayo, A. G. Gayubo, J. Erena, R. Vivanco, and J. Bilbao. "Study of the regeneration stage of the MTG process in a pseudoadiabatic fixed bed reactor". In: *Chemical Engineering Journal* 92.1-3 (2003), pp. 141–150. ISSN: 13858947. DOI: 10.1016/S1385-8947(02)00187-0.

[2] K Andreev, V Kantorová, and J Bongaarts. "Demographic components of future population growth". In: *Technical Paper* 2013/3 (2013).

[3] K. Barbera, F. Bonino, S. Bordiga, T. V. W. Janssens, and P. Beato. "Structure-deactivation relationship for ZSM-5 catalysts governed by framework defects". In: *Journal of Catalysis* 280.2 (2011), pp. 196–205. ISSN: 00219517. DOI: 10.1016/j.jcat.2011.03.016. URL: http://dx.doi.org/10.1016/j.jcat.2011.03.016.

[4] C. H. Bartholomew. "Mechanisms of catalyst deactivation". In: *Applied Catalysis A: General* 212.1-2 (2001), pp. 17–60. ISSN: 0926860X. DOI: 10.1016/S0926-860X(00)00843-7.

[5] P. L. Benito, A. G. Gayubo, A. T. Aguayo, M. Olazar, and J. Bilbao. "Deposition and characteristics of coke over a H-ZSM5 zeolite-based catalyst in the MTG process". In: *Industrial & engineering chemistry research* 35.11 (1996), pp. 3991–3998.

[6] R. J. Berger. *Reactor model in Athena for MTO process with the heat effects*. Tech. rep. Delft: Anaproc, 2015.

[7] F. L. Bleken, K. Barbera, F. Bonino, U. Olsbye, K. P. Lillerud, S. Bordiga, P. Beato, T. V. Janssens, and S. Svelle. "Catalyst deactivation by coke formation in microporous and desilicated zeolite H-ZSM-5 during the conversion of methanol to hydrocarbons". In: *Journal of Catalysis* 307 (2013), pp. 62–73.

[8] D. Chen, K. Moljord, and a. Holmen. "A methanol to olefins review: Diffusion, coke formation and deactivation on SAPO type catalysts". In: *Microporous and Mesoporous Materials* 164 (2012), pp. 239–250. ISSN: 13871811. DOI: 10.1016/j.micromeso.2012.06.046. URL: http://dx.doi.org/10.1016/j.micromeso.2012.06.046.

[9] M. Choi, K. Na, J. Kim, Y. Sakamoto, O. Terasaki, and R. Ryoo. "Stable single-unit-cell nanosheets of zeolite MFI as active and long-lived catalysts". In: *Nature* 461.7261 (2009), pp. 246–249.

[10] M. Choi, K. Na, J. Kim, Y. Sakamoto, O. Terasaki, and R. Ryoo. "Stable single-unit-cell nanosheets of zeolite MFI as active and long-lived catalysts." In: *Nature* 461.7261 (2009), pp. 246–249. ISSN: 0028-0836. DOI: 10.1038/nature08493. URL: http://dx.doi.org/10.1038/nature08288.

[11] A De Lucas, P Canizares, and A Durán. "Improving deactivation behaviour of HZSM-5 catalysts". In: *Applied Catalysis A: General* 206.1 (2001), pp. 87–93.

[12] R. Dessau and R. LaPierre. "On the mechanism of methanol conversion to hydrocarbons over HZSM-5". In: *Journal of Catalysis* 78.1 (1982), pp. 136–141.

[13] J. L. Figueiredo and F. R. Ribeiro. *Catálise Heterogénea*. 2nd. Lisboa: Fundação Calouste Gulbenkian, 2007, pp. 344–368.

[14] S. H. Fogler. *Elements of Chemical Reaction Engineering*. Ed. by P. Hall. 4th. Pearson Education, 2006.

[15] P. Forzatti and L. Lietti. "Catalyst deactivation". In: *Catalysis Today* 52.2-3 (1999), pp. 165–181. ISSN: 09205861. DOI: 10.1016/S0920-5861(99)00074-7.

[16] a. G. Gayubo, A. T. Aguayo, M. Olazar, R. Vivanco, and J. Bilbao. "Kinetics of the irreversible deactivation of the HZSM-5 catalyst in the MTO process". In: *Chemical Engineering Science* 58 (2003), pp. 5239–5249. ISSN: 00092509. DOI: 10.1016/j.ces.2003.08.020.

[17] a. G. Gayubo, a. T. Aguayo, a. Alonso, a. Atutxa, and J. Bilbao. "Reaction scheme and kinetic modelling for the MTO process over a SAPO-18 catalyst". In: *Catalysis Today* 106 (2005), pp. 112–117. ISSN: 09205861. DOI: 10.1016/j.cattod.2005.07.133.

[18] A. G. Gayubo, A. T. Aguayo, M. Castilla, M. Olazar, and J. Bilbao. "Catalyst reactivation kinetics for methanol transformation into hydrocarbons. Expressions for designing reaction-regeneration cycles in isothermal and adiabatic fixed bed reactor". In: *Chemical Engineering Science* 56.17 (2001), pp. 5059–5071. ISSN: 00092509. DOI: 10.1016/S0009-2509(01)00194-4.

[19] J. C. Groen, J. A. Moulijn, and J. Pérez-Ramírez. "Decoupling mesoporosity formation and acidity modification in ZSM-5 zeolites by sequential desilication–dealumination". In: *Microporous and mesoporous materials* 87.2 (2005), pp. 153–161.

[20] IZA. *Database of Zeolite Structures*. URL: http://izasc.biw.kuleuven.be/fmi/xsl/IZA-SC/ft.xsl (visited on 03/22/2015).

[21] A. Izadbakhsh and F. Khorasheh. "Simulation of activity loss of fixed bed catalytic reactor of MTO conversion using percolation theory". In: *Chemical Engineering Science* 66.23 (2011), pp. 6199–6208. ISSN: 00092509. DOI: 10.1016/j.ces.2011.08.047. URL: http://dx.doi.org/10.1016/j.ces.2011.08.047.

[22] T. V. W. Janssens. "A new approach to the modeling of deactivation in the conversion of methanol on zeolite catalysts". In: *Journal of Catalysis* 264.2 (2009), pp. 130–137. ISSN: 00219517. DOI: 10.1016/j.jcat.2009.03.004. URL: http://dx.doi.org/10.1016/j.jcat.2009.03.004.

[23] F. Kaptjein and J. A. Moulijn. "Laboratory Testing of Solid Catalysts". In:

[24] J. Kim, M. Choi, and R. Ryoo. "Effect of mesoporosity against the deactivation of MFI zeolite catalyst during the methanol-to-hydrocarbon conversion process". In: *Journal of Catalysis* 269.1 (2010), pp. 219–228.

[25] P. Losch, M. Boltz, B. Louis, S. Chavan, and U. Olsbye. "Catalyst optimization for enhanced propylene formation in the methanol-to-olefins reaction". In: *Comptes Rendus Chimie* 2014 (2015). ISSN: 16310748. DOI: 10.1016/j.crci.2014.06.007. URL: http://linkinghub.elsevier.com/retrieve/pii/S1631074814001684.

[26] T. Maesen. "The Zeolite Scene - an Overview". In: *Introduction to Zeolite Science and Practice*. Ed. by J. Cejka, V. H. Bekkum, and A. Corma. 3rd. Elsevier, 2007. Chap. 1st.

[27] N.-L. Michels, S. Mitchell, and J. Pérez-Ramírez. "Effects of binders on the performance of shaped hierarchical MFI zeolites in methanol-to-hydrocarbons". In: *ACS Catalysis* 4.8 (2014), pp. 2409–2417.

[28] Morvay Z. K. and D. D. Gvozdenac. "Toolbox 10: Industrial Insulation". In: *Applied Industrial Energy and Environmental Management*. John Wiley & Sons, Ltd, 2008. Chap. Part III: URL: http://www.wiley.com/legacy/wileychi/morvayindustrial/supp/toolbox10.pdf.

[29] J. a. Moulijn, a. E. Van Diepen, and F. Kapteijn. "Catalyst deactivation: Is it predictable? What to do?" In: *Applied Catalysis A: General* 212.1-2 (2001), pp. 3–16. ISSN: 0926860X. DOI: 10.1016/S0926-860X(00)00842-5.

[30] J. a. Moulijn, F. Kapteijn, and G. Mul. *Heterogeneous Catalysis for Chemical Engineers*. August. 2006, p. 286.

[31] S. Müller, Y. Liu, M. Vishnuvarthan, X. Sun, A. C. V. Veen, G. L. Haller, M. Sanchez-sanchez, and J. A. Lercher. "Coke formation and deactivation pathways on H-ZSM-5 in the conversion of methanol to olefins". In: *Journal of Catalysis* 325 (2015), pp. 48–59. DOI: 10.1016/j.jcat.2015.02.013.

[32] G. A. Olah, A. Goeppert, and G. S. Prakash. *Beyond oil and gas: the methanol economy*. John Wiley & Sons, 2009.

[33] G. a. Olah, A. Goeppert, and G. K. S. Prakash. "Beyond Oil and Gas: The Methanol Economy: Second Edition". In: *Beyond Oil and Gas: The Methanol Economy: Second Edition* (2009), pp. 1–334. ISSN: 14337851. DOI: 10.1002/9783527627806.

[34] U. Olsbye, S. Svelle, M. Bjrgen, P. Beato, T. V. W. Janssens, F. Joensen, S. Bordiga, and K. P. Lillerud. "Conversion of methanol to hydrocarbons: How zeolite cavity and pore size controls product selectivity". In: *Angewandte Chemie - International Edition* 51 (2012), pp. 5810–5831. ISSN: 14337851. DOI: 10.1002/anie.201103657.

[35] J. Pérez-Ramírez, R. J. Berger, G. Mul, F. Kapteijn, and J. a. Moulijn. "Six-flow reactor technology a review on fast catalyst screening and kinetic studies". In: *Catalysis Today* 60.1 (2000), pp. 93–109. ISSN: 09205861. DOI: 10.1016/S0920-5861(00)00321-7.

[36] M. Stöcker. "Methanol-to-hydrocarbons: catalytic materials and their behavior". In: *Microporous and Mesoporous Materials* 29 (1999), pp. 3–48. ISSN: 13871811. DOI: 10.1016/S1387-1811(98)00319-9.

[37] A. Taheri Najafabadi, S. Fatemi, M. Sohrabi, and M. Salmasi. "Kinetic modeling and optimization of the operating condition of mto process on sapo-34 catalyst". In: *Journal of Industrial and Engineering Chemistry* 18.1 (2012), pp. 29–37. ISSN: 1226086X. DOI: 10.1016/j.jiec.2011.11.088. URL: http://dx.doi.org/10.1016/j.jiec.2011.11.088.

[38] N. I. o. S. and Technology. *Chemistry WebBook*. 2011. URL: http://webbook.nist.gov/chemistry/.

[39] C. S. Triantafillidis, A. G. Vlessidis, L. Nalbandian, and N. P. Evmiridis. "Effect of the degree and type of the dealumination method on the structural, compositional and acidic characteristics of H-ZSM-5 zeolites". In: *Microporous and Mesoporous Materials* 47.2 (2001), pp. 369–388.

[40] V. Van Speybroeck, K. De Wispelaere, J. Van der Mynsbrugge, M. Vandichel, K. Hemelsoet, and M. Waroquier. "First principle chemical kinetics in zeolites: the methanol-to-olefin process as a case study". In: *Chemical Society Reviews* 43.21 (2014), pp. 7326–7357.

[41] W. Wu, W. Guo, W. Xiao, and M. Luo. "Methanol conversion to olefins (MTO) over H-ZSM-5: Evidence of product distribution governed by methanol conversion". In: *Fuel Processing Technology* 108 (2013), pp. 19–24. ISSN: 03783820. DOI: 10.1016/j.fuproc.2012.05.013. URL: http://dx.doi.org/10.1016/j.fuproc.2012.05.013.

[42] S. Zhang, B. Zhang, Z. Gao, and Y. Han. "Methanol to olefin over Ca-modified HZSM-5 zeolites". In: *Industrial & Engineering Chemistry Research* 49.5 (2010), pp. 2103–2106.

[43] Y. Q. Zhuang, X. Gao, Y. P. Zhu, and Z. H. Luo. "CFD modeling of methanol to olefins process in a fixed-bed reactor". In: *Powder Technology* 221 (2012), pp. 419–430. ISSN: 00325910. DOI: 10.1016/j.powtec.2012.01.041. URL: http://dx.doi.org/10.1016/j.powtec.2012.01.041.

APPENDIX A

Catalytic testing relations

From here after, a resume of the most important catalytic testing conditions and assumptions is presented. These have been the basis for the analysis of plug flow conditions and mass/heat transfer limitations throughout the report.

- In order to neglect the effect of axial dispersion and guarantee plug-flow behaviour, the minimum bed length has to respect the following relation.

$$\frac{L_\mathrm{b}}{d_\mathrm{p}} > \frac{20n}{Bo} \ln\left(\frac{1}{1-X}\right) \tag{A.1}$$

- When it comes to neglecting the wall effects in the gas-solid operation, a minimum reactor diameter has to be satisfied and the following expression must be addressed.

$$\frac{d_\mathrm{t}}{d_\mathrm{p}} > 10 \tag{A.2}$$

- Pressure drop is also a very important parameter and should not to pass over 20% of the operation pressure. It is evaluated using Ergun's expression.

$$\frac{\Delta P_\mathrm{b}}{L_\mathrm{b}} = \frac{150\mu_\mathrm{g}}{{d_\mathrm{p}}^2} \frac{(1-\varepsilon)^2}{\varepsilon^3} u + \frac{1.75\rho_\mathrm{g}}{d_\mathrm{p}} \frac{(1-\varepsilon)}{\varepsilon^3} u^2 < 0.2 \frac{P_\mathrm{tot}}{L_\mathrm{b}} \tag{A.3}$$

- For the calculation of the adiabatic temperature rise, the following expression was used.

$$ATR = \frac{1}{R} \frac{|\Delta H_\mathrm{R}| y_\mathrm{MeOH} X_\mathrm{MeOH}}{C_\mathrm{p,f}} \tag{A.4}$$

- For evaluating the external mass transfer, the Carberry number is evaluated.

$$Ca = \frac{r_{v,obs}}{a' k_f c_b} < \frac{0.05}{|n|} \tag{A.5}$$

- Regarding the internal mass transport, the Weisz-Prater criterion is considered and should be respected.

$$\Phi = \eta\phi^2 = \left(\frac{r_{v,obs}L^2}{D_{eff}C_s}\right)\left(\frac{n+1}{2}\right) < 0.15 \tag{A.6}$$

- For evaluating the extraparticle heat transfer, the following relation must be respected.

$$\gamma\beta_e Ca = \left(\frac{E_a}{RT_b}\right)\left|\frac{(-\Delta H_r)k_f c_b}{hT_b}\right|\left(\frac{r_{v,obs}}{a'k_f c_b}\right) < 0.05 \tag{A.7}$$

- Regarding internal heat transfer, assuming spherical particles, the following relation should also be adressed.

$$\gamma\beta_i(\eta\phi^2) = \left(\frac{Ea}{RT_b}\right)\left|\frac{(-\Delta H_r)D_{eff}C_s}{\lambda_{eff,p}Tb}\right|\left(\frac{r_{v,obs}L^2}{D_{eff}C_s}\right) < 0.1 \tag{A.8}$$

- In order to neglect the effect of radial temperature gradient, the following relation must be respected.

$$\frac{E_a}{RT_w}\left|\frac{r_{V,obs}(-\Delta H_R)d_t^2}{4\lambda_{b,eff}T_w}\right|\left(\frac{1}{8}+\frac{1}{Bi_{h,w}}\frac{d_p}{d_t}\right) < 0.05 \tag{A.9}$$

  Where $\mathrm{Bi_{h,w}}$ is the Biot number for heat transport at the wall: $Bi_{h,w} = \frac{h_w d_p}{\lambda_{b,eff}}$.

- Regarding bed dilution, it should be bear in mind that a certain limited has to be respected in order of not effecting the overall reaction, for example, with bypassing of the catalyst or another negative events. Therefore, the following relation should be addressed.

$$\frac{2.5bd_p}{(1-b)L_b} < 0.05 \tag{A.10}$$

  Where $b = \frac{w_{dil}/\rho_{s,d}}{W_{cat}/\rho_p + W_{dil}/\rho_{s,d}}$

- The observed rate of reaction, $r_{\mathrm{v}}{}^{\mathrm{obs}}$, was changed in the available spreadsheet for the catalytic testing calculations, in order to obtain a conversion of 99.142%. This meant for the observed rate of reaction to be 0.6 $\frac{molMeOH}{kg_{\mathrm{cat}}s}$ in the first set of experiments, and 0.3 $\frac{molMeOH}{kg_{\mathrm{cat}}s}$ in the second set.

For a more complete collection and information about catalytic testing and its associated relations and recommendations, the reader should pay attention to [35] and [23].

APPENDIX B

Catalytic testing results

In this appendix, a resume of the catalytic testing calcuations using the Eurokin's spreadsheet Fixedbed.xls is made.

SUMMARY GAS-SOLID FIXED-BED REACTOR

Overall conclusion: There are one or more aspects causing deviations from intrinsic reaction kinetics at the conditions selected

(The average values from the correlations highlighted green are taken from the worksheet 'Input+calc GS' and these are obtained from the average of all correlations that are valid)

Final conclusions for each aspect:

The assumption of plug-flow regime is	*not allowed*	The effect of mass transport limitations	*cannot be neglected*
The total pressure drop is	*not too high*	The effect of heat transport limitations	*cannot be neglegted*
The amount of inert bed dilution is	*not too high*	(assuming that T(bed) is measured))	

Plug-flow conditions may be assumed and the effects of heat and mass transport limitations can be neglected if there are no values shown in red.

Assumption of plug-flow regime :

O.K. if : bed height / d_p =	*32,585*	>	75,9243	
and if: bed diameter / d_p =	26,8657	>	8	
+ conversion (Berger criterion) =	*0,9914*	<	0,46447	

Pressure drop

Total Δp (Ergun) =	0,07944	<	22,00	[kPa]
This pressure drop corresponds wit	0,07277	[bar/m]		

Amount of dilution in catalyst bed

Dilution = 0	[v/v-tot] < max. allowed dilution =	0,76672		
0	[g/g-tot] < max. allowed dilution =	0,89999		

Conversion	X(MeOH) =	0,99142
Real residence time in the bed	τ_r =	0,07594 s

Adiabatic temperature rise	ΔT(ad)	473,646 K

Mass Transport Limitations :

External (Carberry's number) :	0,00306	<	0,05	
Efficiency (assuming 1st order)	0,99694			
(film thickness =	0,1669	mm)		
Internal (Wheeler-Weisz) :	*1,2925*	<	0,08	
Approximated efficiency (assuming 1st order)	0,62362			

Heat Transport Limitations:

Internal: |ΔT(in pellet)| =	0,06554	[K]	<	2,89795	[K]
External: | ΔT(film) | =	*10,898*	[K]	<	2,89795	[K]
Radial: | ΔT(rad) | =	*153,01*	[K]	<	2,89795	[K]
(However, if T(wall) instead of T(bed) is measured :					
| ΔT(rad) | =	172,5	[K]	<	2,89795	[K])
Axial: | ΔT(ax) | =	*229,062*	[K]	<	2,89795	[K]
Cat-oven: |ΔT(cat-oven|	793,563	[K]	<	2,89795	[K]

This criterion is not applicable if the bed or wall temp. is measured !

Figure B.1: Summary for the experiment at no dilution, 400°C, 0,5 g of ZSM-5 and a WHSV of $8h^{-1}$

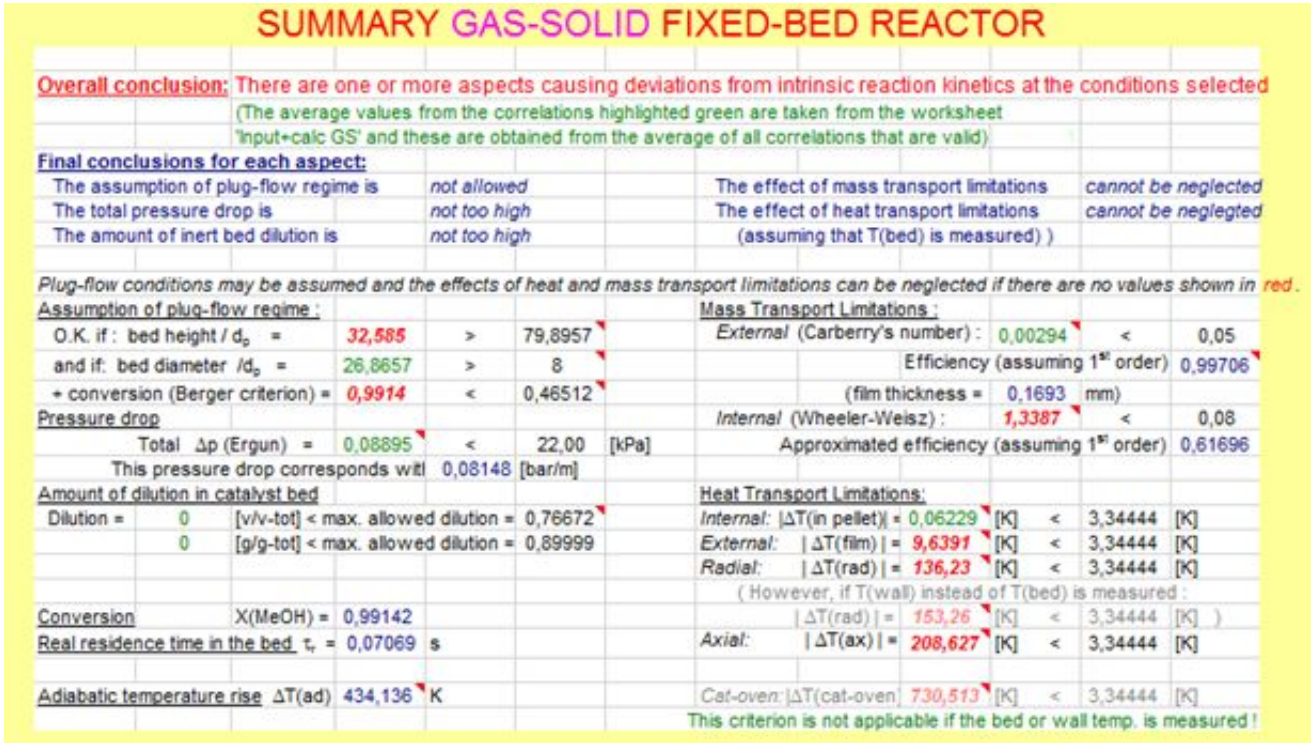

SUMMARY GAS-SOLID FIXED-BED REACTOR

Overall conclusion: There are one or more aspects causing deviations from intrinsic reaction kinetics at the conditions selected

(The average values from the correlations highlighted green are taken from the worksheet 'Input+calc GS' and these are obtained from the average of all correlations that are valid)

Final conclusions for each aspect:

The assumption of plug-flow regime is	*not allowed*	The effect of mass transport limitations	*cannot be neglected*
The total pressure drop is	*not too high*	The effect of heat transport limitations	*cannot be neglegted*
The amount of inert bed dilution is	*not too high*	(assuming that T(bed) is measured))	

Plug-flow conditions may be assumed and the effects of heat and mass transport limitations can be neglected if there are no values shown in red.

Assumption of plug-flow regime :

O.K. if : bed height / d_p =	*32,585*	>	79,8957	
and if: bed diameter /d_p =	26,8657	>	8	
+ conversion (Berger criterion) =	*0,9914*	<	0,46512	

Pressure drop

Total Δp (Ergun) =	0,08895	<	22,00	[kPa]
This pressure drop corresponds with	0,08148			[bar/m]

Amount of dilution in catalyst bed

Dilution = 0	[v/v-tot] < max. allowed dilution =		0,76672	
0	[g/g-tot] < max. allowed dilution =		0,89999	

Conversion	X(MeOH) =	0,99142
Real residence time in the bed	τ_r =	0,07069 s
Adiabatic temperature rise	ΔT(ad)	434,136 K

Mass Transport Limitations :

External (Carberry's number) :	0,00294	<	0,05		
Efficiency (assuming 1st order)			0,99706		
(film thickness =	0,1693	mm)			
Internal (Wheeler-Weisz) :	*1,3387*	<	0,08		
Approximated efficiency (assuming 1st order)			0,61696		

Heat Transport Limitations:

Internal: |ΔT(in pellet)| =	0,06229	[K]	<	3,34444	[K]
External: | ΔT(film) | =	*9,6391*	[K]	<	3,34444	[K]
Radial: | ΔT(rad) | =	*136,23*	[K]	<	3,34444	[K]
(However, if T(wall) instead of T(bed) is measured :					
| ΔT(rad) | =	*153,26*	[K]	<	3,34444	[K])
Axial: | ΔT(ax) | =	*208,627*	[K]	<	3,34444	[K]
Cat-oven: |ΔT(cat-oven)	*730,513*	[K]	<	3,34444	[K]

This criterion is not applicable if the bed or wall temp. is measured !

Figure B.2: Summary for the experiment at no dilution, 450°C, 0,5g ZSM-5 and a WHSV of $8h^{-1}$

SUMMARY GAS-SOLID FIXED-BED REACTOR

Overall conclusion: There are one or more aspects causing deviations from intrinsic reaction kinetics at the conditions selected

(The average values from the correlations highlighted green are taken from the worksheet 'input+calc GS' and these are obtained from the average of all correlations that are valid)

Final conclusions for each aspect:

The assumption of plug-flow regime is	*not allowed*	The effect of mass transport limitations	*cannot be neglected*
The total pressure drop is	*not too high*	The effect of heat transport limitations	*cannot be neglegted*
The amount of inert bed dilution is	*not too high*	(assuming that T(bed) is measured))	

Plug-flow conditions may be assumed and the effects of heat and mass transport limitations can be neglected if there are no values shown in red.

Assumption of plug-flow regime :

O.K. if : bed height / d_p =	*32,585*	>	83,8013	
and if: bed diameter /d_p =	26,8657	>	8	
+ conversion (Berger criterion) =	*0,9914*	<	0,46577	

Pressure drop

Total Δp (Ergun) =	0,09886	<	22,00	[kPa]
This pressure drop corresponds with	0,09057	[bar/m]		

Amount of dilution in catalyst bed

Dilution = 0	[v/v-tot] < max. allowed dilution =	0,76672
0	[g/g-tot] < max. allowed dilution =	0,89999

Conversion	X(MeOH) =	0,99142
Real residence time in the bed	τ_r =	0,06612 s
Adiabatic temperature rise	ΔT(ad)	374,089 K

Mass Transport Limitations :

External (Carberry's number) :	0,00284	<	0,05	
Efficiency (assuming 1st order)	0,99716			
(film thickness =	0,1715	mm)		
Internal (Wheeler-Weisz) :	*1,3833*	<	0,08	
Approximated efficiency (assuming 1st order)	0,61073			

Heat Transport Limitations:

Internal: |ΔT(in pellet)| =	0,05557	[K]	<	3,82291	[K]	
External: | ΔT(film) | =	*8,0342*	[K]	<	3,82291	[K]	
Radial: | ΔT(rad) | =	*114,34*	[K]	<	3,82291	[K]	
(However, if T(wall) instead of T(bed) is measured :						
| ΔT(rad) | =	*128,35*	[K]	<	3,82291	[K]	)
Axial: | ΔT(ax) | =	*178,98*	[K]	<	3,82291	[K]	
Cat-oven: |ΔT(cat-oven|	*633,026*	[K]	<	3,82291	[K]	

This criterion is not applicable if the bed or wall temp. is measured !

Figure B.3: Summary for the experiment at no dilution, 500°C, 0,5g ZSM-5 and a WHSV of $8h^{-1}$

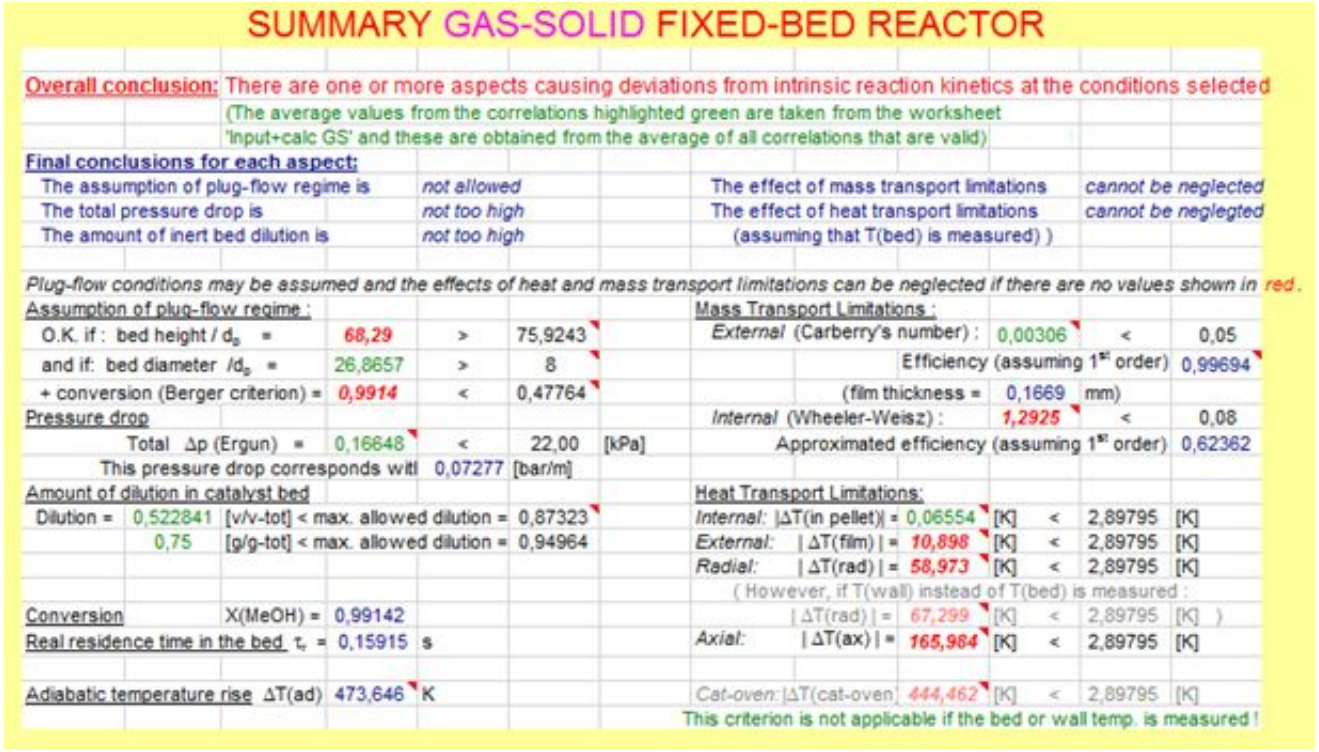

SUMMARY GAS-SOLID FIXED-BED REACTOR

Overall conclusion: There are one or more aspects causing deviations from intrinsic reaction kinetics at the conditions selected

(The average values from the correlations highlighted green are taken from the worksheet 'Input+calc GS' and these are obtained from the average of all correlations that are valid)

Final conclusions for each aspect:

The assumption of plug-flow regime is	*not allowed*	The effect of mass transport limitations	*cannot be neglected*
The total pressure drop is	*not too high*	The effect of heat transport limitations	*cannot be neglegted*
The amount of inert bed dilution is	*not too high*	(assuming that T(bed) is measured))	

Plug-flow conditions may be assumed and the effects of heat and mass transport limitations can be neglected if there are no values shown in red.

Assumption of plug-flow regime :

O.K. if : bed height / d_p =	*68,29*	>	75,9243	
and if: bed diameter / d_p =	26,8657	>	8	
+ conversion (Berger criterion) =	*0,9914*	<	0,47764	

Pressure drop

Total Δp (Ergun) =	0,16648	<	22,00	[kPa]
This pressure drop corresponds with	0,07277	[bar/m]		

Amount of dilution in catalyst bed

Dilution = 0,522841	[v/v-tot] < max. allowed dilution =	0,87323		
0,75	[g/g-tot] < max. allowed dilution =	0,94964		

Conversion	X(MeOH) =	0,99142
Real residence time in the bed	τ_r =	0,15915 s
Adiabatic temperature rise	ΔT(ad)	473,646 K

Mass Transport Limitations :

External (Carberry's number) :	0,00306	<	0,05	
Efficiency (assuming 1st order)	0,99694			
(film thickness =	0,1669	mm)		
Internal (Wheeler-Weisz) :	*1,2925*	<	0,08	
Approximated efficiency (assuming 1st order)	0,62362			

Heat Transport Limitations:

Internal: |ΔT(in pellet)| =	0,06554	[K]	<	2,89795	[K]	
External: | ΔT(film) | =	*10,898*	[K]	<	2,89795	[K]	
Radial: | ΔT(rad) | =	*58,973*	[K]	<	2,89795	[K]	
(However, if T(wall) instead of T(bed) is measured :						
| ΔT(rad) | =	67,299	[K]	<	2,89795	[K]	)
Axial: | ΔT(ax) | =	*165,984*	[K]	<	2,89795	[K]	
Cat-oven: |ΔT(cat-oven)	444,462	[K]	<	2,89795	[K]	

This criterion is not applicable if the bed or wall temp. is measured !

Figure B.4: Summary for the experiment at a 3:1 dilution, 400°C, 0,5g of ZSM-5 and a WHSV of $8h^{-1}$

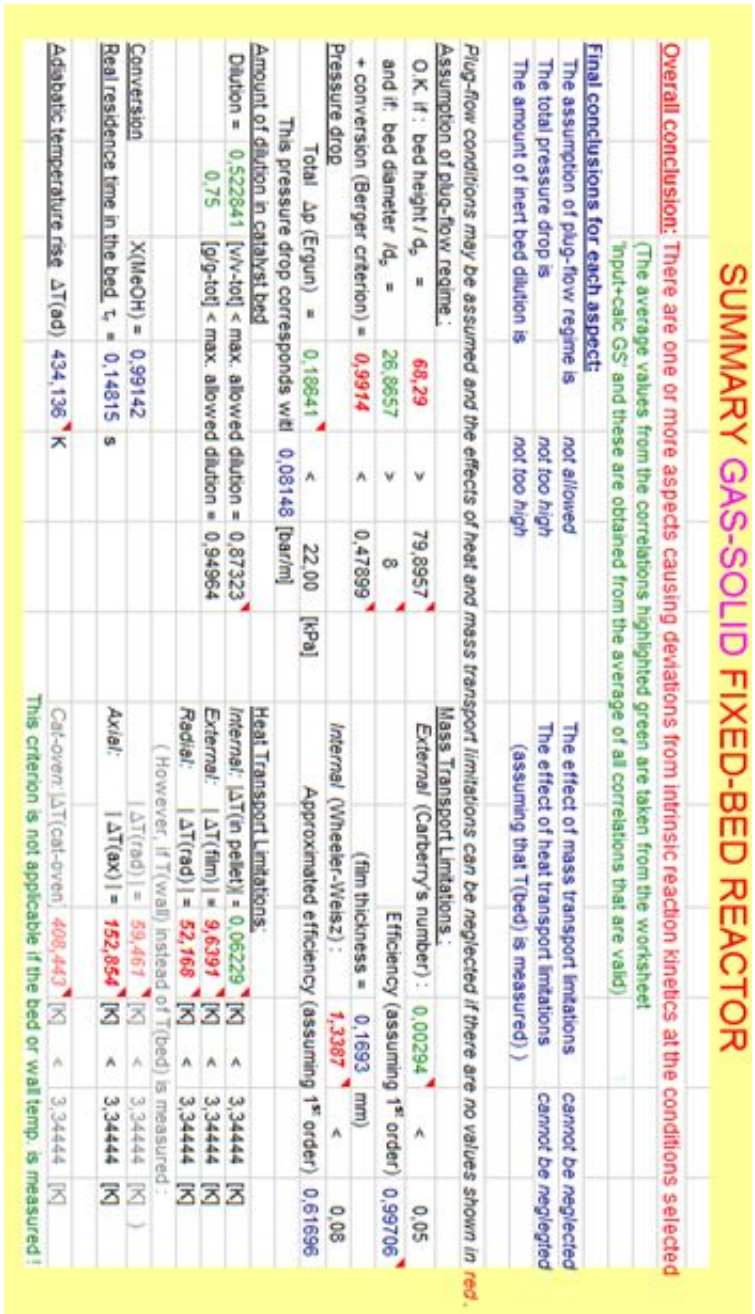

Figure B.5: Summary for the experiment at a 3:1 dilution, 450°C, 0,5g of ZSM-5 and a WHSV of $8h^{-1}$

SUMMARY GAS-SOLID FIXED-BED REACTOR

Overall conclusion: There are one or more aspects causing deviations from intrinsic reaction kinetics at the conditions selected

(The average values from the correlations highlighted green are taken from the worksheet 'Input+calc GS' and these are obtained from the average of all correlations that are valid)

Final conclusions for each aspect:

The assumption of plug-flow regime is	*allowed*	The effect of mass transport limitations	*cannot be neglected*
The total pressure drop is	*not too high*	The effect of heat transport limitations	*cannot be neglegted*
The amount of inert bed dilution is	*not too high*	(assuming that T(bed) is measured))	

Plug-flow conditions may be assumed and the effects of heat and mass transport limitations can be neglected if there are no values shown in red.

Assumption of plug-flow regime :

O.K. if : bed height / d_p =	103,994	>	75,9243	
and if: bed diameter /d_p =	26,8657	>	8	
+ conversion (Berger criterion) =	***0,9914***	<	0,4905	
Pressure drop				
Total Δp (Ergun) =	0,25352	<	22,00	[kPa]
This pressure drop corresponds with	0,07277			[bar/m]
Amount of dilution in catalyst bed				
Dilution = 0,686665 [v/v-tot] < max. allowed dilution =			0,91296	
0,857143 [g/g-tot] < max. allowed dilution =			0,96635	
Conversion X(MeOH) =	0,99142			
Real residence time in the bed τ_r =	0,24237	s		
Adiabatic temperature rise ΔT(ad)	473,646	K		

Mass Transport Limitations :

External (Carberry's number) :	0,00306	<	0,05	
Efficiency (assuming 1st order)	0,99694			
(film thickness =	0,1669	mm)		
Internal (Wheeler-Weisz) :	***1,2925***	<	0,08	
Approximated efficiency (assuming 1st order)	0,62362			

Heat Transport Limitations:

Internal: |ΔT(in pellet)| =	0,06554	[K]	<	2,89795	[K]
External: | ΔT(film) | =	***10,898***	[K]	<	2,89795	[K]
Radial: | ΔT(rad) | =	***35,152***	[K]	<	2,89795	[K]
(However, if T(wall) instead of T(bed) is measured :					
| ΔT(rad) | =	*40,278*	[K]	<	2,89795	[K])
Axial: | ΔT(ax) | =	***126,697***	[K]	<	2,89795	[K]
Cat-oven: |ΔT(cat-oven)	*313,155*	[K]	<	2,89795	[K]

This criterion is not applicable if the bed or wall temp. is measured !

Figure B.6: Summary for the experiment at a 6:1 dilution, 400°C, 0,5g of ZSM-5 and a WHSV of $8h^{-1}$

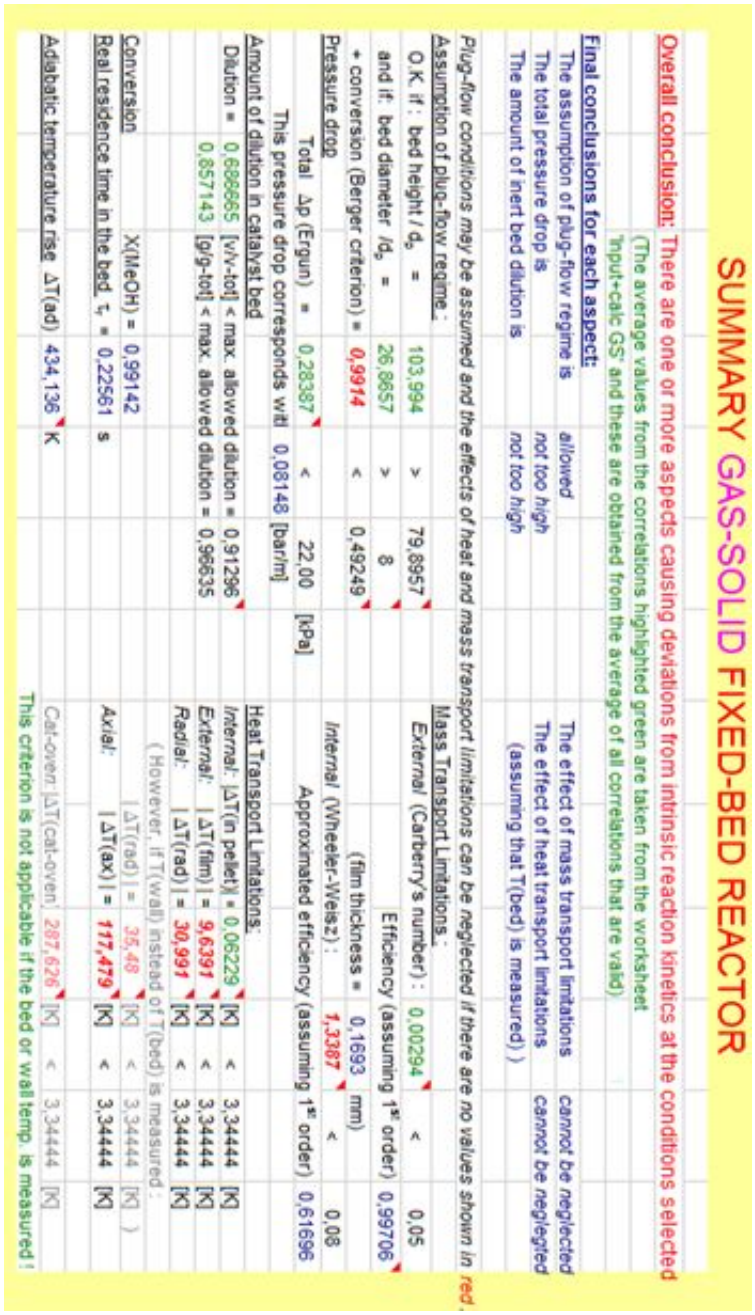

SUMMARY GAS-SOLID FIXED-BED REACTOR

Overall conclusion: There are one or more aspects causing deviations from intrinsic reaction kinetics at the conditions selected

(The average values from the correlations highlighted green are taken from the worksheet 'Input+calc GS' and these are obtained from the average of all correlations that are valid)

Final conclusions for each aspect:

The assumption of plug-flow regime is	*allowed*				The effect of mass transport limitations			*cannot be neglected*
The total pressure drop is	*not too high*				The effect of heat transport limitations			*cannot be neglected*
The amount of inert bed dilution is	*not too high*				(assuming that T(bed) is measured))			

Plug-flow conditions may be assumed and the effects of heat and mass transport limitations can be neglected if there are no values shown in red.

Assumption of plug-flow regime :					Mass Transport Limitations :					
O.K. if : bed height / d_p =	103,994	>	79,8957		*External* (Carberry's number) :	0,00294	<	0,05	
and if: bed diameter /d_p =	26,8657	>	8		Efficiency (assuming 1st order)	0,99706			
+ conversion (Berger criterion) =	0,9914	<	0,49249		(film thickness =	0,1693	mm)		
Pressure drop					*Internal* (Wheeler-Weisz) :	1,3387	<	0,08	
Total Δp (Ergun) =	0,28387	<	22,00	[kPa]	Approximated efficiency (assuming 1st order)			0,61696	
This pressure drop corresponds with	0,08148	[bar/m]							
Amount of dilution in catalyst bed					Heat Transport Limitations:				
Dilution = 0,888665 [v/v-tot] < max. allowed dilution =	0,91296				*Internal:* |ΔT(in pellet)| =	0,06229	[K]	<	3,34444 [K]
0,857143 [g/g-tot] < max. allowed dilution =	0,96635				*External:* | ΔT(film) | =	9,6391	[K]	<	3,34444 [K]
					Radial: | ΔT(rad) | =	30,991	[K]	<	3,34444 [K]
					(However, if T(wall) instead of T(bed) is measured :				
					| ΔT(rad) | =	35,48	[K]	<	3,34444 [K])
Conversion X(MeOH) =	0,99142				*Axial:* | ΔT(ax) | =	117,479	[K]	<	3,34444 [K]
Real residence time in the bed, τ_r =	0,22561	s							
					Cat-oven: |ΔT(cat-oven)|	287,626	[K]	<	3,34444 [K]
Adiabatic temperature rise ΔT(ad)	434,136	K							

This criterion is not applicable if the bed or wall temp. is measured !

Figure B.7: Summary for the experiment at a 6:1 dilution, 450°C, 0,5g of ZSM-5 and a WHSV of $8h^{-1}$

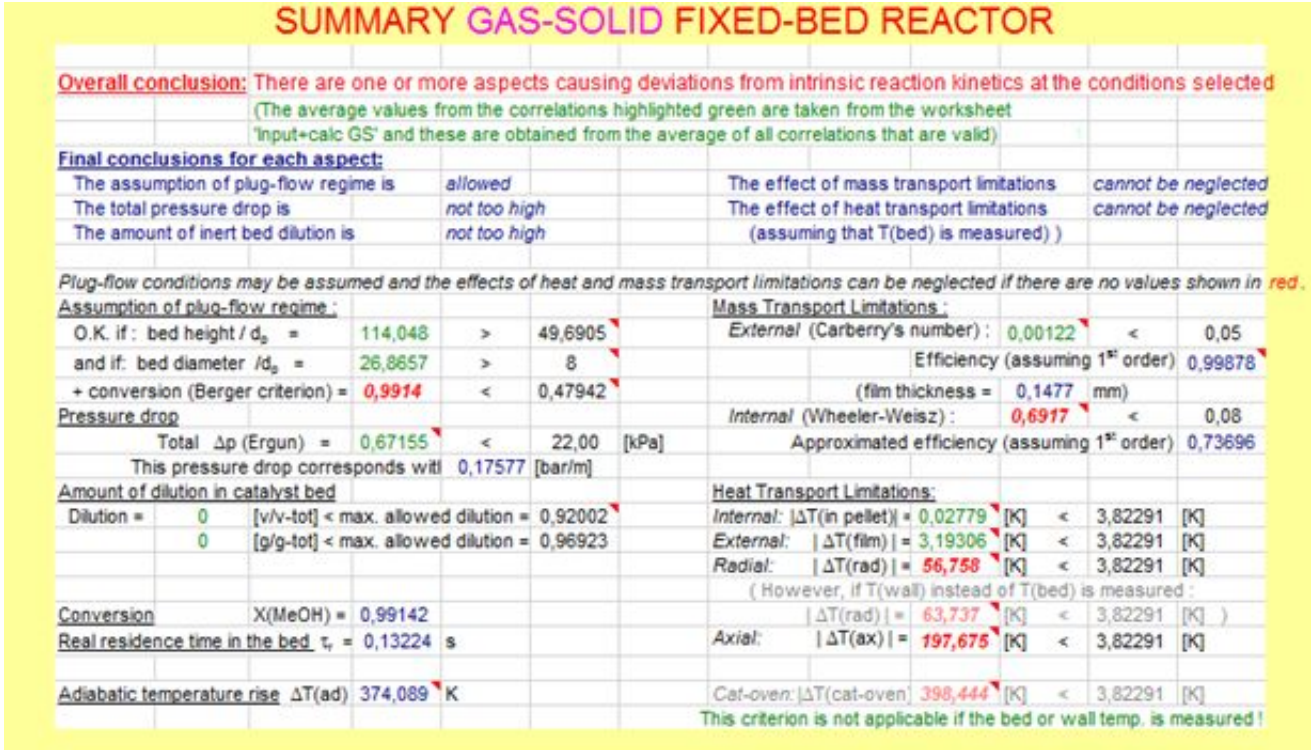

SUMMARY GAS-SOLID FIXED-BED REACTOR

Overall conclusion: There are one or more aspects causing deviations from intrinsic reaction kinetics at the conditions selected

(The average values from the correlations highlighted green are taken from the worksheet 'Input+calc GS' and these are obtained from the average of all correlations that are valid)

Final conclusions for each aspect:

The assumption of plug-flow regime is	*allowed*	The effect of mass transport limitations	*cannot be neglected*
The total pressure drop is	*not too high*	The effect of heat transport limitations	*cannot be neglected*
The amount of inert bed dilution is	*not too high*	(assuming that T(bed) is measured))	

Plug-flow conditions may be assumed and the effects of heat and mass transport limitations can be neglected if there are no values shown in red.

Assumption of plug-flow regime :

O.K. if : bed height / d_p =	114,048	>	49,6905	
and if: bed diameter / d_p =	26,8657	>	8	
+ conversion (Berger criterion) =	*0,9914*	<	0,47942	
Pressure drop				
Total Δp (Ergun) =	0,67155	<	22,00	[kPa]
This pressure drop corresponds with	0,17577	[bar/m]		

Amount of dilution in catalyst bed

Dilution = 0	[v/v-tot] < max. allowed dilution =	0,92002		
0	[g/g-tot] < max. allowed dilution =	0,96923		

Conversion	X(MeOH) =	0,99142
Real residence time in the bed	τ_r =	0,13224 s
Adiabatic temperature rise	ΔT(ad)	374,089 K

Mass Transport Limitations :

External (Carberry's number) :	0,00122	<	0,05	
Efficiency (assuming 1st order)	0,99878			
(film thickness =	0,1477	mm)		
Internal (Wheeler-Weisz) :	*0,6917*	<	0,08	
Approximated efficiency (assuming 1st order)	0,73696			

Heat Transport Limitations:

Internal: |ΔT(in pellet)| =	0,02779	[K]	<	3,82291	[K]
External: | ΔT(film) | =	3,19306	[K]	<	3,82291	[K]
Radial: | ΔT(rad) | =	*56,758*	[K]	<	3,82291	[K]
(However, if T(wall) instead of T(bed) is measured :					
| ΔT(rad) | =	63,737	[K]	<	3,82291	[K])
Axial: | ΔT(ax) | =	*197,675*	[K]	<	3,82291	[K]
Cat-oven: |ΔT(cat-oven)	398,444	[K]	<	3,82291	[K]

This criterion is not applicable if the bed or wall temp. is measured !

Figure B.8: Summary for the experiment at a no dilution, 500°C, 1,75g of ZSM-5 and a WHSV of $4h^{-1}$ (the three thermocouples' experiment)

APPENDIX C

Preliminar calculations for the adiabatic temperature rise

For calculating the adiabatic temperature rise, it was necessary to calculate the global enthalpy of reaction for the three different temperatures. Therefore, several steps were taken in order to reach those values, which are going to be described for the order that they were performed.

1. First of all, the representative reactions for the hydrocarbon-pool system have to be defined. These are chosen based on the results on selectivity for the developed experiments. These have been already presented in the body of this report and correspond to Equations 4.1, 4.2, 4.3, 4.4, 4.5 and 4.6.

2. Then, based on the enthalpy of formation for each chemical species [38], the standard enthalpy of reaction for each one of the five considered.

Table C.1: Standard enthalpies of reaction for the six representative in this hydrocarbon-pool system

R1	R2	R3	R4	R5	R6
-21.18 kJ/mol	-90.07 kJ/mol	-215.18 kJ/mol	-147.14 kJ/mol	-207.68 kJ/mol	-445.58 kJ/mol

3. Moreover, what is need is the enthalpy of reaction for each different temperature of operation. Hence, one can firstly consider the already calculated standard enthalpy of reaction at 25℃, and them sum the integral from the reference to the desired temperature, over the product of the heat capacity by the number of moles, for each chemical species and for each reaction considered.

$$\Delta H_{\mathrm{R}} = \left(\sum_i n_{\mathrm{i}} \int_{25℃}^{T_{\mathrm{reac}}} Cp_{\mathrm{i}} \mathrm{d}T\right)_{prod} - \left(\sum_i n_{\mathrm{i}} \int_{25℃}^{T_{\mathrm{reac}}} Cp_{\mathrm{i}} \mathrm{d}T\right)_{reag} + \Delta H^{\circ}{}_{\mathrm{R}} \quad \text{(C.1)}$$

Regarding the calculation of $\int_{25°C}^{T_{reac}} Cp_i dt$, the values for heat capacity between the limits of integration were taken for each chemical species, from the software Aspen Plus®.

4. Finally, each enthalpy of reaction is multiplied by the molar fraction of the related species on the stream, which is function of the selectivity. The sum of all these parcels is equal to the global enthalpy of reaction, for each temperature used, and those can be found in the Table 4.3.

APPENDIX D

Calculations for the global heat transfer coefficient

To evaluate the heat transfer conditions between the reactor and the sequential walls that separate it from the inside of the hotbox, the global heat transfer coefficient for this system was calculate. For the fact that it is the case of an consecutive insulation barriers, it was chosen the expression from Morvay and Gvozdenac [28].

$$\begin{aligned}\frac{1}{U} &= \sum R = R_{\text{in}} + R_{\text{w,glass}} + R_{\text{ins,SS}} + R_{\text{ins,ext}} + R_{\text{out}} \\ &= \frac{D_4}{D_1 h_{\text{in}}} + \frac{D_4 \ln\left(\frac{D_2}{D_1}\right)}{2k_{\text{w}}} + \frac{D_4 \ln\left(\frac{D_3}{D_2}\right)}{2k_{\text{in,SS}}} + \frac{D_4 \ln\left(\frac{D_4}{D_3}\right)}{2k_{\text{ins,ext}}} + \frac{1}{h_{\text{out}}}\end{aligned} \tag{D.1}$$

Where w refers to wall, SS to stainless steel, ext to external insulation, which are all the insulation resistances found in this system. These can be related by the following Figure D.1.

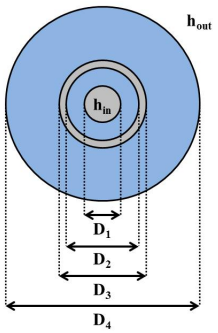

Figure D.1: Schematic representation on close-up over the experimental set-up, regarding the reaction tube and the insulation system over it

In Table D.1, one can find a resume of the characteristics for the gas mixture that travels along the reactor, considering the normal composition of nitrogen, olefins, paraffins

and water, for 1 bar, 500 °C and a WHSV = 4 h^{-1}. An average of the pellet size was considered (335 μm), as well as a bed of 1.75 g.

Table D.1: Resume of the flow characteristics of the gas mixture admitted to the reactor

Cp	1.60 kJ/kgK
Average MW	24.11 g/mol
Density	0.41 kg/m^3
Thermal conductivity	$6.70.10^{-5}$ kW/mK
Velocity	0.02 m/s
Viscosity	$3.27.10^{-5}$ Pa.s
Re	2.40
Rep	$8.92.10^{-2}$
Pr	$7.82.10^{-1}$
Nu	$6.25.10^{-3}$

Nonetheless, for the stagnated air surrounding the external wall, also the necessary parameters were considered and calculated, which can be found in the Table D.2.

Table D.2: Resume of the characteristics of the stagnated air surrounding the external wall

Tinf	423.15 K
Tw	748.15 K
Cp	1.01 kJ/kgK
Conductivity	0.03 W/mK
Viscosity	$2.39.10^{-5}$ Pa.s
Pr	0.70
Gr	935054.50
Ra	654963.74

The expressions for internal and external individual heat transfer coefficients were given by Kapteijn and Moulijn [23].

$$Nu = \frac{h_{\text{in}} d_{\text{p}}}{\lambda_{\text{f}}} \tag{D.2}$$

Where for gases,

$$Nu \approx 0.07 Re_{\text{p}} \tag{D.3}$$

$$\frac{h_{\text{out}} L}{k_{\text{g,out}}} = 0.68 + \frac{0.0670 Ra^{1/4}}{\left[1 + \left(\frac{0.492}{Pr}\right)^{9/16}\right]^{4/9}} \tag{D.4}$$

In Table D.3, a resume of the insulation thermal conductivity is found.

Where,

$$Gr = \frac{9.8 \frac{1}{T} \left(T_{\text{w}} - T_{\infty}\right) L^3}{\frac{\mu_{\text{ex}} k_{\text{g,ex}}}{\rho_{\text{ex}} Cp_{\text{g,ex}}}} \tag{D.5}$$

Table D.3: Thermal conductivity for the three insulation materials involved in the reaction system

Wall	SS	External insulation
1.05 W/mK	18 W/mK	2.07 W/mK

$$Ra = Gr.Pr \tag{D.6}$$

Finally, one can find both individual heat transfer coefficients and calculate the global heat transfer coefficient (Table D.4).

Table D.4: Resume on heat transfer coefficients

$\mathbf{h_{in}}$	$\mathbf{h_{out}}$	U
$9.97 \cdot 10^{-1}$ W/m^{2}K	1.48 W/m^{2}K	1.29 W/m^{2}K